Adaptive Parallel Interference Cancellation Receivers with Diversity Combining for Multicarrier DS CDMA Systems

WANG HUAHUI

A THESIS SUBMITTED

FOR THE DEGREE OF MASTER OF ENGINEERING

DEPARTMENT OF ELECTRICAL AND COMPUTER ENGINEERING

NATIONAL UNIVERSITY OF SINGAPORE

2003

Acknowledgement

I am taking this opportunity to express my sincere gratitude towards Dr. Chew Yong Huat, Yen Kai and Ang Kay Wee. Their trust and the help in my research work are not the only things that I have been grateful for. I always take it as my pride to have such good luck to be able to work under their supervision. Their help has really smoothed my studies and my life in Singapore.

I also want to thank my colleagues Dauglas, Bijay and Stephen; they have offered me a lot of help in my English writing. To my friends Erji, Haiming, Yixin and Sunyan, I owe my gratitude for their encouragement when I was down in my spirits and for the fun they have brought to me. Without them, life would not be so interesting for a man who does not know how to entertain himself.

Also I would like to thank those who taught me how to play games. Although I have not found the sense of what they have declared - that games can allowed me to expand my creative mind to new boundaries I never had, I would thank them in the same manner for helping me have another way of entertainment. Since they are all shy men, I would be quite understandable not to mention their names here; just remember them in my heart …

The rest of my thanksgivings are for my family - my parents, my sister and my brother-in-law. They are always wishing the best for me. Their love and never-ending support are things that I treasure the most.

Table of Contents

Nomenclature

AMPS	Advanced Mobile Phone Service
APIC	Adaptive Parallel Interference Cancellation
AWGN	Additive White Gaussian Noise
BER	Bit Error Rate
BPSK	Binary Phase Shift Keying
CAI	Common Air Interface
CDMA	Code Division Multiple Access
CPIC	Conventional Parallel Interference Cancellation
DAMPS	Digital Advanced Mobile Phone Service
DCA	Dynamic Channel Assignment
DETC	Digital European Cordless Telecommunications
DFE	Decision-feedback Equalization
DSP	Digital Signal Processing
EGC	Equal Gain Combining
ETSI	European Telecommunication Standardization Institute
FDD	Frequency Division Duplexing
FDM	Frequency Division Multiplexing
FDMA	Frequency Division Multiple Access
FFT	*Fast Fourier Transform*
FM	Frequency Modulation
FSK	Frequency Shift Keying
GMSK	Gaussian Minimum Shift Keying

GSM	Global System for Mobile Communications
IC	Interference Cancellation
ICI	Inter-chip Interference
IDFT	*Inverse Discrete Fourier Transform*
IFFT	*Inverse Fast Fourier Transform*
ISDN	Integrated Services Digital Network
ISI	Inter-symbol Interference
LEC	Local Exchange Carrier
LMS	Least-mean-square
MAI	Multiple Access Interference
MCM	Multicarrier Modulation
MC-CDMA	Multicarrier Code Division Multiple Access
MC-DS-CDMA	Multicarrier Direct Sequence Code Division Multiple Access
MF	Matched Filter
MIPS	Million-Instructions-Per-Second
MLS	Maximum-likelihood Sequence
MMSE Minimum	Mean-squared Error
MSE	Mean Square Error
MRC	Maximal Ratio Combining
MSK	Minimum Phase Keying
MT-CDMA	Multitone Code Division Multiple Access
NMT	Nordic Mobile Telephone
NTT	Nippon Telephone and Telegraph
OFDM	Orthogonal Frequency Division Duplexing
PACS	Personal Access Communications Services

pdf	Probability Density Function
PG	Processing Gain
PHS	Personal Handyphone System
PIC	Parallel Interference Cancellation
PN	Pseudo-noise
QPSK	Quadrature Phase Shift Keying
RHS	Right Hand Side
SC-DS-CDMA	Single Carrier Direct Sequence Code Division Multiple Access
SD	Selection Diversity
SIC	Serial or Successive Interference Cancellation
SNR	Signal to Noise Ratio
S/P	Serial to Parallel
SS	Spread Spectrum
TACS	Total Access Communications System
TDD	Time Division Duplexing
TDMA	Time Division Multiple Access
UMTS	Universal Mobile Telecommunication Systems
WACS	Wireless Access Communications Systems
WCDMA	Wideband Code division Multiple Access
ZF	Zero-forcing

List of Figures

List of Tables

Summary

Orthogonal frequency division multiplexing (OFDM) combined with code division multiple access (CDMA) makes the multicarrier (MC-) CDMA systems one of the promising candidates for the next generation mobile communication systems because of their high bandwidth efficiency and robustness against the hostile nature of the broadband radio channel. In this thesis, one of the three basic MC CDMA systems, namely MC-DS-CDMA system, is under investigation.

Although MC CDMA systems are promising candidates for high bit rate data transmission and can have high capacity in selective fading channel, the multiple access interference (MAI) problems inherent to the single-carrier (SC-) DS-CDMA system also exists and is the limitation to its achievable capacity. In this thesis, a parallel interference cancellation (PIC) receiver with an adaptive MAI estimation stage is proposed for both synchronous and asynchronous MC-DS-CDMA systems. Since the synchronous system has a much simpler receiver structure compared to the asynchronous one, in order to simplify the exposition and the analysis, this thesis places more emphasize on the synchronous case. Simulations are carried out in various conditions to investigate the performance of the synchronous system. The investigation has shown that by using MRC to exploit the frequency diversity provided by the MC-DS-CDMA system, the proposed adaptive PIC (APIC) receiver has significant performance improvement over the matched filter (MF) and the conventional PIC (CPIC) receiver.

Derivations of the closed form expressions for the bit error rate (BER) of the APIC detectors (both synchronous and asynchronous) are also presented in this thesis. The simulation results have been found to agree well with the theory.

Chapter 1

Introduction

The birth of wireless communications can be traced back to the year 1897, when Guglielmo Marconi demonstrated the radio's capability by continuously contacting sailing ships over a distance of about 18 kilometers. Since then, throughout more than 100 years of its history, wireless communication has enjoyed its growth all over the world, especially in the past two decades. Today mobile telephony has penetrated our daily lives and it will surely have an even greater impact on our lives in the next decade.

The perspective of the future wireless personal communications is to allow a user to gain access to the capabilities of the global network at any time regardless of its location or mobility. This goal is difficult to meet due to the implications on both the radio interface and the protocol structure. Cellular and cordless telephony systems have both begun the process to fulfill this goal but yet do not allow total wireless communications. Cellular systems currently are limited to voice and low-speed data within areas covered by base stations. On the other hand, the cordless telephony can provide high-speed services only over short distances and in an environment of less mobility.

1.1 Evolution of Mobile Communications

1.1.1 Cellular Radio

In the 70's of the last century, the cellular concept developed by Bell Laboratories made it feasible to provide wireless communications to the entire population. With the development of highly reliable, miniature, solid-state radio frequency hardware in the 1970's, the wireless communications era was born [1]. The cellular systems in the early 1980's using analog technologies were referred to as first-generation cellular. The initial system realization in the United States was known as AMPS, for Advanced Mobile Phone Service. Systems similar to AMPS were soon deployed internationally, for example TACS (Total Access Communications System) and NMT (Nordic Mobile Telephone) in Europe, and NTT (Nippon Telephone and Telegraph) system in Japan. These systems used analog frequency modulation (FM) for speech transmission and frequency shift keying (FSK) for signaling. Individual calls use different frequencies. This way of sharing the spectrum is called frequency division multiple access (FDMA).

Analog cellular systems were followed in the early 1990's by second-generation digital technologies. Digitization allows the use of time division multiple access (TDMA) and code division multiple access (CDMA) as alternatives to FDMA. With TDMA, the usage of each radio channel is partitioned into multiple timeslots and each user is assigned a specific frequency/timeslot combination. With CDMA (which uses direct sequence spreading), a frequency channel is used simultaneously by multiple mobiles in a given cell and the signals are distinguished by spreading them with different codes [2]. The use of TDMA and CDMA offers advantages such as the capability of supporting much higher number of mobile subscribers within a given frequency allocation, better voice quality, lower complexity and flexible support of

new services. The digital cellular approach has become a real success. The vast majority of the subscribers are based on the Global System for Mobile Communications (GSM) Standard proposed by Europe, which today is deployed in more than 100 countries. The GSM standard uses Gaussian minimum shift keying (GMSK) modulation scheme and it adopts TDMA as the access technology. A very important contribution of GSM is that it brought forward strict criteria on its interfaces such that every system following such criteria can be compatible with each other. Another feature of GSM is that it has an interface compatible with Integrated Services Digital Network (ISDN). Other systems that are based on TDMA are Digital AMPS (DAMPS) in North America and Personal Digital Cellular (PDC) in Japan. DAMPS system, based on the IS-54 standard, operates in the same spectrum with the existing AMPS systems, thus making the standard IS-54 a "dual mode" standard that provides for both analog (AMPS) and digital operations. Another standard by North America is IS-95, which is based on narrow-band CDMA and can operate in AMPS mode as well. This standard has very attractive features such as increased capacity, eliminating the need for planning frequency assignments to cells and flexibility for accommodating different transmission rates.

Cellular systems such as GSM and DAMPS are optimized for wide-area coverage, giving bit rates around 100 kbps. Further development will be capable of providing user data rates of up to 384kbps. However, for a whole range of communication services involving voice, data, video, and images, even higher data rate is required. Standardization is ongoing for third-generation systems in the European Telecommunication Standardization Institute (ETSI), under the project name Universal Mobile Telecommunication Systems (UMTS) and in the International Telecommunications Union (ITU), where it is called IMT2000. UMTS aims to deliver

wide-area/high-mobility data rates of 384 kbps, and up to 2 Mbps for local-area/low-mobility coverage. ETSI decided to adopt the UMTS standard based on a new wideband (W)CDMA technology which supports instant access to wireless multimedia optimized for packet-switched data. This is a totally new approach to CDMA technology and inherently different from previously proposed narrowband CDMA systems such as IS-95. This WCDMA technology is also adopted by Japan. Another proposal is the CDMA2000 by the United States, which is compatible with IS-95 CDMA. Tests have shown that CDMA becomes a more attractive technology when it is wideband [3].

Wireless service providers are slowly beginning to deploy third-generation (3G) cellular services. As access technology increases, voice, video, multimedia, and broadband data services are becoming integrated into the same network. The hope once envisioned for 3G as a true broadband service has all but dwindled away. Maintaining the possible 2Mbps data rate in the standard, 3G systems that were built so far can only realistically achieve 384kbps rates. To achieve the goals of a true broadband cellular service, the systems have to make the leap to a fourth-generation (4G) network. 4G is intended to provide high speed, high capacity, low cost per bit and IP based services. The goal is to achieve data rates of up to 20Mbps, even when used in scenarios such as a vehicle traveling at 200km per hour. New techniques, however, are needed to make this happen. 4G does not have any standard specifications yet, but it is clear that some standardization is in process.

1.1.2 Cordless Telephony

Being another important part of the wireless personal communications, cordless telephony systems have a similar development as cellular mobile communications, evolving from analog systems to digital ones.

First-generation analog cordless telephones originated in the United States from the 1980's. Their popularity continued for a considerable time mainly due to their low cost. A standard referred to as CT1 was developed in Europe after the cordless telephones were imported into the continent. CT1 historically is a coexistent standard rather than an interoperable standard, which has the consequence that equipment from different manufacturers are typically incompatible. The demand for these devices is fairly small due to the inherent deficiencies such as very limited operating range (on the order of 10 m), low capacity, poor voice quality and incompatibility to the digital services. Therefore, the work on the digital cordless telephones was stimulated.

Digital technologies such as speech coding were exploited in the second-generation of the cordless telephone systems, the standard of which is referred to as CT2/Common Air Interface (CAI). The most salient features of that standard are the digital transmission format and the use of time division duplexing (TDD). Dynamic Channel Assignment (DCA) technique is exploited to increase the spectrum efficiency. Voice quality is also improved. CT2 was prompted as a Telepoint standard. Telepoint networks use cordless base stations to provide wireless pay phone services. Incoming calls are not supported with the basic service. A Canadian enhancement of the CT2/CAI, called CT2+, is designed to provide some of the missing mobility management functions such as enabling the Telepoint subscribers to receive calls. In summary, the family of CT2 standards is an attractive option for cordless and Telepoint systems optimized with respect to cost.

In 1992, ETSI proposed a third-generation cordless telephone standard, named Digital European Cordless Telecommunications (DECT). DECT uses TDMA and TDD. It is designed as a flexible interface to provide cost-effective communication service to high user densities in picocells. It supports multiple bearer channels for speech and data transmission, handover, location registration and paging. Functionally, it is closer to a cellular system than to a classical cordless telephone. Japan prompted a Personal Handyphone System (PHS) in 1993. It also uses TDMA and TDD. DECT is designed for operation in an uncoordinated environment, which means that the base stations need not be synchronized. Unlike DECT, however, PHS provided dedicated control channels. In the United States, Bell Communications Research (Bellcore) developed an air interface for Wireless Access Communications Systems (WACS). The WACS air interface is similar to the digital cordless interfaces with the exception that it uses frequency division duplexing (FDD) instead of TDD. It is intended to provide wireless connectivity to the local exchange carrier (LEC) and is designed with low-speed portable applications and small-cell systems. The attributes of WACS and PHS have been combined to create an industry standard proposal for Personal Access Communications Services (PACS), which is proposed as a “low-tier” air interface for the licensed portion of the 2-GHz spectrum.

In general, the digital cordless systems are optimized for low-complexity equipment and high-quality speech in a quasi-static environment. Conversely, the digital cellular air interfaces are geared toward maximizing bandwidth efficiency and frequency reuse in a macrocellular and high-speed fading environment. This is achieved at the price of increased complexity at the terminal and the base station.

1.2 Problems in Future Mobile Communications

The long-term goal of mobile communications in Europe is to unify the worlds of cellular, cordless, low-end wireless LAN, private mobile radio and paging. The idea of this Universal Mobile Telecommunications System (UMTS) is to provide the same type of services everywhere, with the only limitation being that the available data rate may depend on the location and the load of the system. This goal is difficult to meet. A major issue is the provision of high data rates. However, if higher data rate is to be achieved at a fairly low cost, the cordless functions can be taken over by the cellular radio services.

As we have mentioned, 4G is intended to provide mobile data at rates of more than 20Mbps. A promising underlying technology for 4G's physical layer is Orthogonal Frequency Division Multiplexing (OFDM). OFDM is a special form of multicarrier modulation (MCM), in which a signal is split into several narrowband channels and modulated at different frequencies. Mostly, OFDM systems are designed such that each subcarrier is narrow enough in bandwidth in order to experience frequency-flat fading.

It is well known that the mobile communication channel is usually characterized by "multipath reception" and such a multipath propagation causes inter-symbol interference (ISI) as well as inter-chip interference (ICI), if the channel delay spread exceeds the symbol duration [4]-[6] and CDMA is deplyed. Fast data transmission becomes unrealistic in the presence of ISI and ICI. A technique combining both OFDM and CDMA, which is called multicarrier CDMA (MC-CDMA), was proposed to suppress ISI and ICI. Since OFDM is a parallel transmission, it reduces the chip rate per carrier and the broad bandwidth can be divided into narrowband carriers for system realization [5]. Because of their high bandwidth efficiency and robustness against the

hostile nature of the broadband radio channel, great research interest has been attracted so far.

In MC-CDMA, similar to single carrier (SC-) CDMA systems, the users are multiplexed with orthogonal codes to distinguish between the multiple users simultaneously accessing the system. Therefore, as with 3G systems, 4G systems have to deal with issues of multiple access interference (MAI), which is the most significant limiting factor on the performance and the capacity of the SC-CDMA system.

1.3 Contribution of the Thesis

This thesis focuses on MAI cancellation for multicarrier direct sequence CDMA (MC-DS-CDMA) system, which is one of the three basic types of multicarrier CDMA systems that will be described further in the next chapter. Adaptive parallel interference cancellation (APIC) receivers are proposed for both synchronous and asynchronous MC-DS-CDMA systems. By taking advantage of combining techniques such as maximal ratio combining (MRC), the diversity provided by the MC-DS-CDMA system can be exploited to improve the bit error probability and increase the user/data capacity. The performance behaviour under different conditions is studied in detail for the synchronous system.

In this contribution, a simple but accurate closed form expression for the bit error rate (BER) of the proposed adaptive PIC (APIC) receiver is derived. The simulation results agree well with the theoretical ones obtained from the expression. For comparison purpose, the expressions for the matched filter (MF) and the conventional PIC (CPIC) receiver are also presented. Investigation has shown that the proposed APIC receiver outperforms the MF and the CPIC receivers under fading.

1.4 Organization of the Thesis

The outline of the thesis is as follows.

Chapter 2 describes the three basic types of multicarrier CDMA systems by introducing their transmission and reception schemes as well as analyzing their corresponding frequency spectra. Features such as the subcarrier frequency separation and the required bandwidth will be compared between these systems. The advantages and the disadvantages of these systems will also be highlighted in one table for easy reference. Despite the various differences between these systems, all of them have one attractive feature in common: the robustness against frequency selective fading. This is the motivation of prompting these schemes. However, the inherited MAI problem from conventional CDMA systems also limits the performance of these multicarrier CDMA systems which stimulated the investigation on the varieties of multiuser detection schemes.

Chapter 3 investigates the various detection schemes. The first scheme adopted in the implementation of CDMA receivers is the matched filter (MF) receiver. It is a single-user detector which treats the interference from other users as noise and takes no measures to mitigate these interferences. The multiuser detection techniques become popular because they can suppress the MAI through a joint detection which takes advantage of the other users' information to combat the interferences instead of just treating them as the white Gaussian noise. Maximum likelihood sequence detector is one with the best performance. However the exponentially increasing complexity with the number of users makes it impractical to realize. Suboptimal detectors have been proposed to offer a trade off between the performance and the complexity. Two categories of suboptimal detectors will be reviewed in this chapter, namely, linear detectors and subtractive detectors. A simplified synchronous CDMA system model is

invoked in order to make the introduction of these detection schemes concise. At the end of the chapter, all these techniques are compared with respect to the performance and complexity.

In Chapter 4, the PIC scheme with an MAI estimation stage is proposed for the synchronous MC-DS-CDMA system. The structure of the proposed receiver and the derivation of the BER expression for this scheme are highlighted in this chapter. For comparison purpose, the performance of the MF receiver as well as the conventional PIC receiver is also analyzed. Actually, the MF receiver constitutes the initial stage of this adaptive PIC receiver, and if the adaptive weights of the MAI estimation stage of the proposed scheme are fixed at 1, the adaptive PIC receiver turns into the conventional PIC receiver.

In Chapter 5, the performance of the adaptive PIC receiver in the synchronous system is investigated under different conditions. Monte Carlo simulations are performed to analyze the BER performance of both the SC-DS-CDMA system and MC-DS-CDMA system. The Jakes' model is adopted to shape the characteristics of the channel. Assumptions such as perfect channel estimation, power control and time-invariant channel are made to simplify the cases. In this chapter, the MC-DS-CDMA system is investigated from various aspects such as its comparison with the SC-DS-CDMA system and its inherent diversity property. More emphases are placed on the studies of the performance of the adaptive PIC receiver under different conditions: the BER versus capacity, BER versus SNR, and the influences on the performance of the receiver by selecting the step-size and initial weights of the adaptive algorithm, and so on and so forth.

Chapter 6 has a parallel structure with Chapter 4. The topic is on the structure of the adaptive PIC receiver for the asynchronous MC-DS-CDMA system and the

theoretical analysis on its BER performance. The reason for a different structure from that of the synchronous case is that the synchronous receiver is a subcarrier-based program, which uses the demodulated signal on each subcarrier as the reference, while in asynchronous case, such a scheme becomes impossible due to the time offset between users.

Chapter 7 draws to the closure of this thesis by giving the conclusion and the comments for the future work.

Chapter 2

Multicarrier CDMA Systems

Multicarrier CDMA (MC-CDMA) systems are robust against frequency selective fading, which is a severe problem in mobile radio communications, because it tends to lead to burst errors in high-speed data transmission. The robustness of these systems can be explained as they are actually OFDM systems with a CDMA overlay. CDMA has a lot of attractive advantages yet it is subject to the frequency selective fading. This is compensated by OFDM, in which a signal is split into several narrowband channels and modulated at different frequencies. Most OFDM systems are designed such that each subcarrier is narrow enough in bandwidth in order to experience frequency-flat fading.

2.1 Code Division Multiple Access (CDMA)

CDMA is a multiple access scheme that differentiates between users by assigning unique codes to these users. Although, the users sharing the spectrum overlap in time and frequency, the receiver is able to sift each user's information from other users by correlating the received signal with the spreading code given to that particular user. The spreading codes are designed such that the cross-correlation of spreading codes of any two users is almost zero. This allows multiple users to transmit in this same band without interfering with each other. However, the receiver has full information about

the spreading codes of each user and can de-spread the corresponding narrowband signal of each user. Encoding the user information with its unique code usually enlarges the user's signal bandwidth. Hence this technique is also known as spread spectrum (SS).

CDMA has numerous inherent advantages that are derived from the spectral spreading. To spread a signal, the most common way is Direct Sequence Spread Spectrum (DS-SS). In DS-SS, a narrowband signal is multiplied by a pseudo-noise (PN) spreading sequence. The rate of the spreading codes, usually referred to as the chip rate, is faster than the data rate of the signal. Consequently, the chip duration T_c is smaller than the bit duration of the original signal, which is denoted as T_b.

The ratio of bit duration T_b to chip duration T_c is called Processing Gain (PG). It is desirable to have a high PG in order to support higher number of users, because the higher the PG the more the narrowband interference rejection capability. The spreading of the signal in Additive White Gaussian Noise (AWGN) causes the signal amplitude to be lower than when not spreading thereby hiding the information signal. [7] gives a systematic overview of CDMA system and describes how the PG can improve the capability of narrowband interference rejection.

The effect of multiplying the signal in time by a spreading code is equivalent in the frequency domain to convolving the frequency responses of both signals and the spectral property of the spreading codes such that it spreads the signal. Figure 2.1 shows the time domain analysis of multiplying a signal by a higher rate PN sequence. The frequency domain analysis is shown in Figure 2.2.

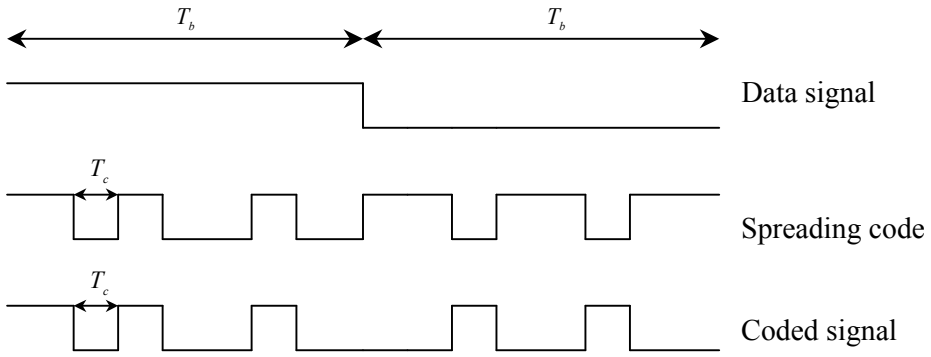

Figure 2.1 Spreading the signal with a higher rate spreading code (time domain)

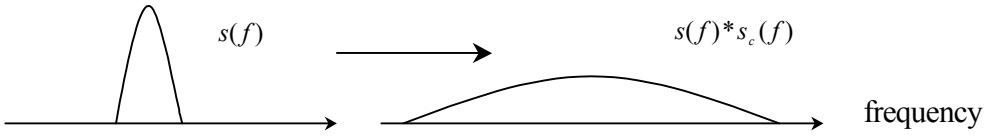

Figure 2.2 Spreading the signal with a higher rate spreading code (frequency domain)

CDMA has numerous inherent advantages that are derived from the spectral spreading. These advantages, to name a few, include: improved capacity, narrow-band interference rejection, ISI rejection and higher privacy, etc. In the hostile mobile communications channel, frequency selective multipath fading causes severe degradation in a CDMA system. As mentioned in [4], multipath propagation causes ICI in the DS-SS-CDMA system and severe ISI in high data rate systems if the channel delay spread exceeds the symbol duration. Due to the severe ICI and the difficulty in synchronization, conventional CDMA has been designed only for low- or medium-bit-rate transmission. OFDM is the technique prompted to solve this problem.

2.2 Orthogonal Frequency Division Multiplexing (OFDM)

Orthogonal Frequency Division Multiplexing (OFDM) is a multicarrier modulation (MCM) scheme [8-10]. In an OFDM system, multiple data symbols are transmitted in parallel using different subcarriers. These subcarriers have overlapping spectra, but their signal waveforms are specifically chosen to be orthogonal. Mostly, OFDM systems are designed such that each subcarrier is narrow enough in bandwidth in order to experience frequency-flat fading. This also ensures that the subcarriers remain orthogonal when received over a moderately frequency selective but time-invariant channel.

The orthogonality of the carriers means that each carrier has an integer number of cycles over a symbol period. Due to this, the spectrum of each carrier has a null at the center frequency of each of the other carriers in the system. This results in no interference between the carriers, allowing them to be spaced as close as theoretically possible. This overcomes the problem of overhead carrier spacing required in FDMA systems. OFDM is the most efficient FDM scheme, since no guard frequency band between adjacent carriers is necessary.

Since OFDM is a parallel transmission approach, it has the advantage of spreading out a fade over many symbols. As explained in [10], this can effectively randomize the burst errors caused by the Rayleigh fading, so that instead of several adjacent symbols being completely destroyed, many symbols are only slightly distorted. This allows precise reconstruction of a majority of them.

Another significant advantage of OFDM is that the task of pulse forming and modulation can be performed by a simple *Inverse Discrete Fourier Transform* (IDFT) which can be implemented very efficiently as an *Inverse Fast Fourier Transform* (IFFT). Accordingly in the receiver only an FFT is needed to reverse this operation.

In summary, OFDM systems are attractive with such advantages as:

- It mitigates the ISI at no or insignificant bandwidth cost, as mentioned previously.
- It reduces the speed of the signal processing because of the longer symbol period.
- The transmitter and receiver complexity becomes a signal-processing task.

It can provide frequency diversity if the same data is repeated on the multiple sub-carriers. A diversity combining technique such as maximal ratio combining (MRC) or equal gain combining (EGC) can be used in collecting the signal energy from the various carriers. This will definitely increase the signal to noise ratio at the receiver although at the cost of bandwidth since the data rate is reduces.

2.3 Multicarrier CDMA Systems

The first MC-CDMA system was proposed by N. Yee, J-P. Linnartz and G. Fettweis [11] in 1993. Shortly after that, the MC-DS-CDMA was proposed by V. DaSilva and E. S. Sousa [12] and the MT-CDMA by Vandendorpe [13]. Although there are other versions of the MC-CDMA system, these three systems are the foundation for which other MC-CDMA systems are built. An overview of MC-CDMA systems was presented by S. Hara and R. Prasad in [14].

2.3.1 MC-CDMA spread in Frequency domain

Transmitter

In this design, the incoming bit stream is copied to N symbols. These N symbols are each modulated onto a different orthogonal carrier frequency. However, the spreading of the symbol is done in the frequency domain before modulating to the carrier frequencies. Each carrier is spread with a chip from the spreading sequence belonging

to the user who sends the data. This is equivalent to performing a *N*-point serial to parallel (S/P) conversion after a data stream has been spread by the spreading sequence. Spreading codes like the Hadamard Walsh codes [7] have been shown to be optimum in maintaining orthogonality between subcarriers and reducing inter-modulation in non-linear amplifiers. All the *N* modulated signals are summed together and transmitted. The transmitter structure is shown in Figure 2.3.

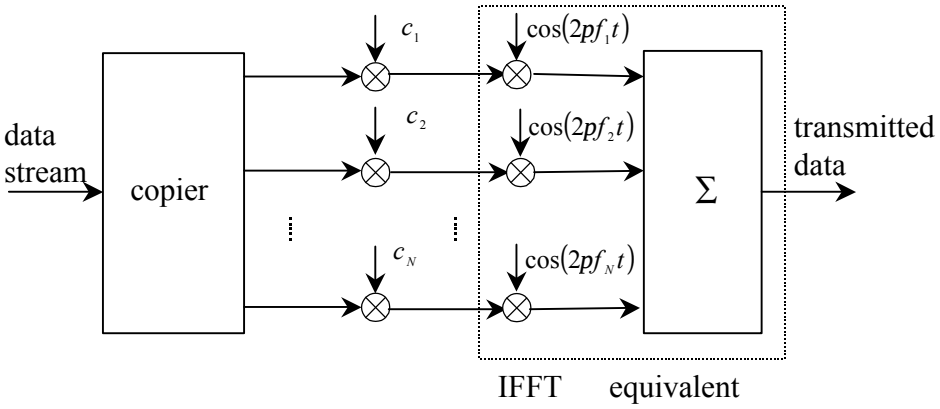

Figure 2.3 MC-CDMA transmitter

The modulation operation shown in the dashed box of Figure 2.3 is equivalent to the IFFT operation, as proven in Appendix A. Thus a simplified MC-CDMA system can be implemented by replacing the modulators with the IFFT operation.

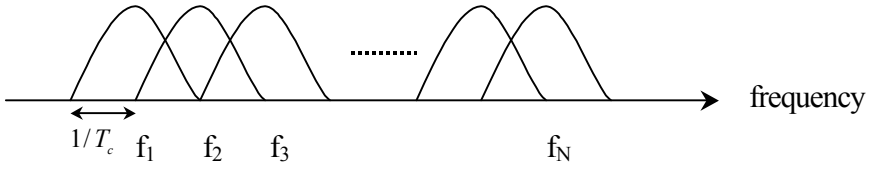

Figure 2.4 Frequency spectrum of transmitted signal

The frequency spectrum of the MC-CDMA signal is shown in Figure 2.4. Suppose the PG of the system is *G* and the incoming data duration for one bit is T_s, the chip duration on each subcarrier is then $T_c = T_s N / G$. The required bandwidth for this MC-

CDMA scheme is $(N+1)G/(T_s N)$. In the illustration of Figure 2.3 and 2.4, the assumption of $N = G$ is made. However, this is not necessary. If the original data steam is first converted into P parallel sequences and then each sequence is mapped onto G subcarriers, we have $N = PG$.

Receiver

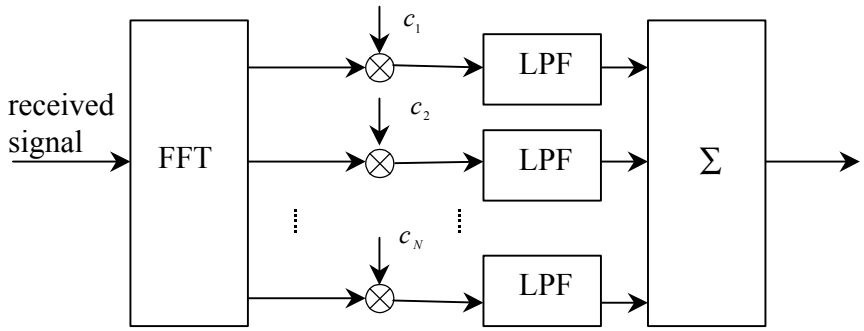

Figure 2.5 MC-CDMA receiver

The receiver reverses the operation of the transmitter. First, the received signal is demodulated, equivalent to multiplying this signal with the N orthogonal carrier frequencies and then low pass filtered the resulting signals. Demodulation for the simplified MC-CDMA can be implemented by performing the FFT operation at the receiver on the received signal. The demodulated signals are each multiplied with the same spreading sequence used at the transmitter. Next, the receiver will attempt to detect the transmitted data symbols from the despread signals. Figure 2.5 shows the receiver design of the MC-CDMA.

2.3.2 MC-DS-CDMA

This scheme is the combination of time domain spreading and multicarrier modulation, originally proposed in [12] for an uplink communication channel, because the introduction of OFDM signaling into DS-CDMA scheme is effective for the

establishment of a quasi-synchronous channel.

Transmitter

The transmitter spreads the S/P converted data streams using a given spreading code in the time domain so that the resulting spectrum of each subcarrier can satisfy the orthogonal condition with the minimum frequency separation, as shown in Figure 2.6. The symbols modulated on the N subcarriers are summed together before being transmitted over the channel. The N subcarriers can be overlapping as in the conventional OFDM. For the overlapping case, the adjacent subcarriers are separated by $1/T_c$, where $T_c = T_s N / G$. The frequency spectrum is same with Figure 2.4.

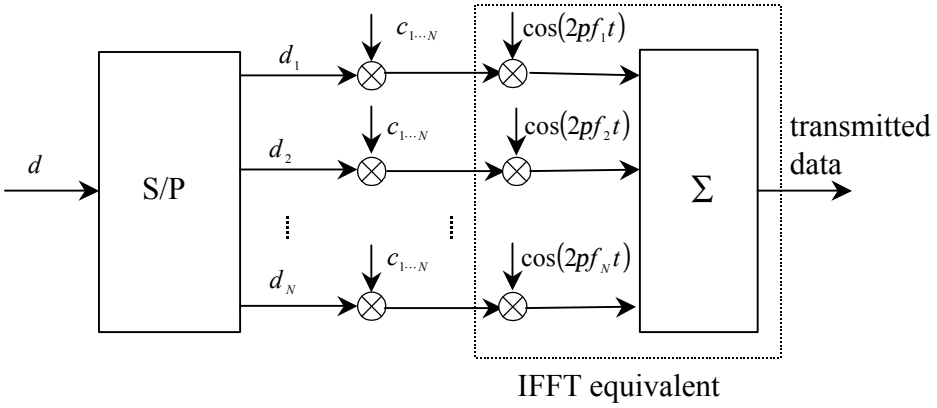

Figure 2.6 MC-DS-CDMA transmitter

Receiver

At the receiver, the signals are demodulated by the N carriers and despread with the user's spreading sequence. The receiver design is shown in Figure 2.7.

As in the MC-CDMA, the MC-DS-CDMA transmitter with overlapping carrier frequency spectra can be implemented with an IFFT operation and the receiver by an FFT operation while the nonoverlapping carrier frequency spectra (similar to the

frequency division multiplexing (FDM) multicarrier modulation) requires N modulators.

It is important to note that each symbol in the MC-DS-CDMA is spread in time by the same spreading sequence per carrier while in the MC-CDMA, each symbol is spread by a spreading sequence in frequency but one chip per carrier.

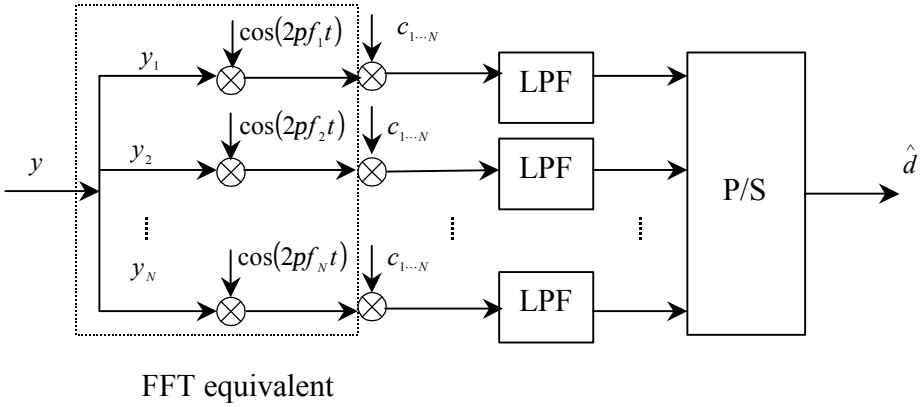

Figure 2.7 MC-DS-CDMA receiver

2.3.3 Multi-tone (MT-) CDMA

Transmitter

MT-CDMA is similar to the MC-DS-CDMA with the incoming bit stream divided into N different bit streams, after which the spreading of each stream is done in time with a long spreading sequence aimed at maintaining a constant bandwidth for each of the subcarriers. The ratio of the length of spreading codes, r, to the number of sub-carriers is kept constant. The relationship is $r / N = G$, where G has been denoted previously as being the PG of the MC-CDMA and MC-DS-CDMA system.

The MT-CDMA transmitter has the same structure as that of MC-DS-CDMA. Its only difference from MC-DS-CDMA is that the spectrum of each subcarrier prior to the spreading operation satisfies the orthogonal condition which subsequently loses the orthogonal quality after spreading. This is achieved by separating the subcarrier

frequency with $1/NT_s$ and keeping the chip duration as $NT_s/r = T_s/G$, where r is the PG of the MT-CDMA system. Note that in MC-DS-CDMA system, the chip duration is $T_s N/G$ and the separation of the subcarrier is $G/T_s N$. Loss of orthogonality after spreading results in ICI. In the frequency domain, the bandwidth of each subcarrier after spreading is larger than the coherence bandwidth of the channel, therefore, with a high PG, each subcarrier will experience frequency selective fading. The frequency domain spectrum is shown in Figure 2.8.

Figure 2.8 Frequency spectrum of transmitted MT-CDMA signal receiver

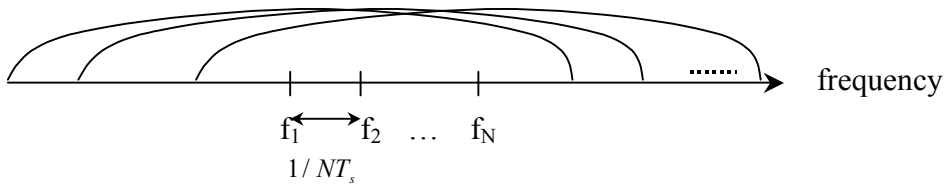

The transmitter design is performed using the same data mapping and spreading (in time) as in the MC-DS-CDMA except that longer codes are used to spread each subcarrier signal such that it experiences frequency selective fading. Therefore, a Rake receiver [15] or other multiuser detector can be used at the receiver. It is important to note that because the adjacent carriers are separated by $1/NT_s$ the N modulators/ demodulators in the transmitter/receiver can be implemented by the IFFT/FFT. The receiver designs using analog modulators are shown in Figure 2.9.

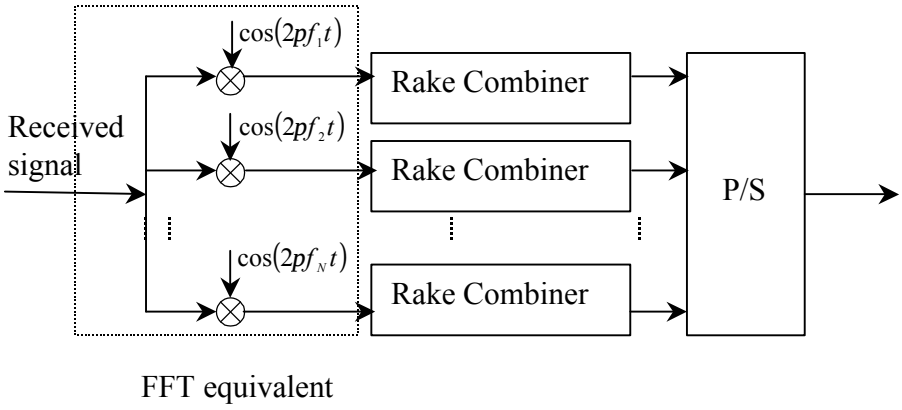

Figure 2.9 MT-CDMA receiver

2.4 Systems Comparison

Based on the description highlighted previously, a comparison on the features among the three systems is shown in Table 2.1. The rectangular pulse shape is assumed in all the systems. The required bandwidths of MC-CDMA and MC-DS-CDMA are almost half of that of the DS-CDMA and the bandwidth of MT-CDMA is comparable with that of DS-CDMA scheme.

Table 2.1 Features of various CDMA systems

	DS-CDMA	MC-CDMA	MC-DS-CDMA	MT-CDMA
Number of subcarriers	1	N	N	N
Processing gain (PG)	*G*	*G*	G	GN
Symbolduration at subcarrier	T_s	T_sN / G	T_sN	T_sN

Chip duration	T_s / G	T_sN / G	T_sN / G	T_s / G
Frequency separation		$1 / T_s$	$G/(T_sN)$	$1/(NT_s)$
Required bandwidth	$2G / T_s$	$(N+1)G / (NT_s)$	$(N+1)G / (NT_s)$	$(2GN+N-1) / (NT_s)$

Table 2.2 briefly compares the advantages and disadvantages of three multicarrier CDMA systems.

Table 2.2 Comparison of advantages and disadvantages of three multicarrier CDMA systems

Scheme	Advantages	Disadvantages
MC-CDMA	▪ Transmits multiple carrier per symbol, therefore diversity combining can be applied.	▪ Implementation complexity is higher than other MC-CDMA systems.
MC-DS-CDMA	▪ Good for uplink transmission because it does not require that the users be synchronized. ▪ Diversity combining can be applied when the same symbol is repeated on all the sub-carriers. ▪ It needs fewer carriers and thus allows the processing gain (PG) to be increased ▪ Robust to timing errors and frequency offsets.	▪ Performance is not as good as MC-CDMA
MT-CDMA	▪ Longer spreading codes result in a reduction in self-interference and multiple access interference as compared to those experienced in conventional CDMA system. ▪ Detection can be done non-coherently.	▪ The modulated signal experience ISI and ICI.

Chapter 3

Multiuser Detection Schemes

3.1 Limitations of the Conventional CDMA Systems

As described in [16], a conventional CDMA detector treats each user separately as a signal, with the other users considered as either interference, or noise. The detection of the desired signal is protected against the interference due to the other users by the inherent interference suppression capability of CDMA, measured by the processing gain. The interference suppression capability is, however, not unlimited and when the number of the users increases, the equivalent noise results in degradation of performance, i.e., increasing bit error rate or frame error rate.

Even if the number of users is not too large, some users may be received at such a high signal level that a lower power user may be swamped out. This is the near-far effect: users near the receiver are received at higher powers as compared to those far away, and those further away suffer a degradation in performance. Even if users are at a same distance from the receiver, there can be an effective near-far effect because some users may be received during a deep fade. There are thus two key limits to CDMA systems:

- All users interfere with all other users and the interferences add to cause a performance degradation.

- The near-far problem is serious and tight power control, with attendant complexity, is needed to combat it.

3.2 Interferences and Solutions in the Conventional DS-CDMA Systems

Signal distortion affects the performance of wireless communications systems. This distortion can be broadly classified into two categories: One is the ISI, caused by delays of the signal propagated through different paths, and the other is the MAI. In a CDMA system, a number of users simultaneously transmit information over a common channel using different code sequences. In the reverse link, transmitters send information independently. Therefore, signals from different users arrive asynchronously at the receiver so the cross-correlation between the received signals of different users is nonzero or quite high. This results in the MAI, which is the most significant limiting factor on the performance and the capacity of the CDMA system.

3.2.1 ISI cancellation

If ISI is left uncompensated, it will cause high error rates. The solution to the ISI problem is to design a receiver that employs a means for compensating or reducing the ISI in the received signal. The compensator for the ISI is called an *equalizer*.

Three types of equalization methods are treated in [15], chapter 10. One is based on the maximum-likelihood sequence (MLS) detection criterion, which is optimum from a probability of error viewpoint but the computational complexity grows exponentially with the length of the channel time dispersion. A second equalization method is sub-optimal and is called *linear equalization.* It is based on the use of a linear filter with adjustable coefficients. To reduce the ISI, several criteria such as zero-forcing (ZF) and minimum mean square error (MMSE) are introduced in the

literature. The third equalization method that is described exploits the use of previously detected symbols to suppress the ISI in the present symbol being detected, and it is called *decision-feedback* equalization (DFE). Detailed description of equalizers is presented in [15].

3.2.2 MAI Cancellation

In a conventional CDMA system, all users interfere with each other. Potentially significant capacity increases and near-far resistance can theoretically be achieved if the negative effect that each user has on others can be cancelled. A more fundamental view of this is multiuser detection, in which all users are considered as signals for each other, they are all being used for their mutual benefit by joint detection [16].

There is a great deal of similarity between multiuser and ISI channels. This point is made where the asynchronous *K*-user channel is identified with the periodically time-varying ISI channel with memory *K-1*; that is, overlapping ISI symbols can be considered to be separate users. Therefore, several of the multiuser detectors have equalizer counterparts, such as the MLS, ZF, MMSE, and DFE. Some of the multiuser detectors are designed to eliminate both ISI and MAI.

Since the cancellation of MAI is most important in improving the performance and capacity of the CDMA system, a detailed description of MAI cancellation is presented below. A significant amount of research has been done in trying to mitigate the effect of MAI; much of this work had been done in the area of multiuser detection. In multiuser detection, code and timing information of multiple users are used to better detect each individual user. A succinct introduction of multiuser detection can be found in [15], chapter 15. S. Verd? [1984] gives a systematic description of the multiuser detection in [17].

3.3 Multiuser Detection Schemes for Conventional DS-CDMA Systems

3.3.1 Simplified DS-CDMA System Model

Although the channel is generally asynchronous in realistic applications, a simple synchronous model is adopted in this section, in order to make the discussion succinct and the concept easier to understand. In a synchronous channel, all bits of all users are aligned in time while in the asynchronous channel signals are randomly delayed from one another.

Further assumptions include the additive white Gaussian noise (AWGN) channel and the zero phases of all carriers, i.e., baseband signal processing. Since in synchronous transmission, each interferer produces exactly one symbol which interferes with the desired symbol, in AWGN channel, it is sufficient to consider the signal received in one signal interval, say $0 \le t \le T$.

Assuming K users in a synchronous DS-CDMA system with binary phase-shift keying (BPSK) modulation, the received baseband signal is given as

$$r(t) = \sum_{k=1}^{K} A_k b_k s_k(t) + n(t), t \in [0, T] \tag{3.1}$$

where T is the inverse of the data rate, A_k, b_k and $s_k(t)$ are the amplitude, modulated data and signature code waveform of the kth user, respectively, and $n(t)$ is the AWGN noise with zero mean and double-sided power spectral density of $N_0/2$. The binary data b_k takes on ± 1 value and A_k^2 is referred to as the energy of the kth user; $s_k(t)$ is zero outside of $[0, T]$ and is normalized so as to have unit energy

$$\int_0^T s_k(t)^2 \, dt = 1 \tag{3.2}$$

The crosscorrelation between the signature waveforms is defined as

$$r_{i,j} = \int_0^T s_i(t)s_j(t)dt \tag{3.3}$$

The crosscorrelation matrix can be written as

$$\mathbf{R} = \{r_{i,j}\} \tag{3.4}$$

3.3.2 Single-User Matched Filter (Conventional Detector)

Matched filter (MF) is the demodulator that was first adopted in the implementation of CDMA receivers. In the multiuser detection literature, it is frequently referred to as the *conventional detector*.

In conventional detection, the receiver for each user consists of a demodulator that correlates (or matched filters) the received signal with the signature sequence of the users and passes the correlator output to the detector, which makes a decision based on the presence of the other users in the channel or, equivalently, assumes that the aggregate noise plus interference is white and Gaussian.

As shown in Figure 3.1, the output of the matched filter for user *k* is

$$y_k = \int_0^T r(t)s_k(t)dt \tag{3.5}$$

Using (3.1) and (3.3), the output of the *k*th matched filter can be expressed as

$$\begin{aligned} y_k &= A_k b_k + \sum_{j \neq k} A_j b_j r_{jk} + n_k \\ &= A_k b_k + MAI_k + n_k \end{aligned} \tag{3.6}$$

where

$$n_k = \int_0^T n(t)s_k(t)dt \tag{3.7}$$

is a Gaussian random variable with zero mean and variance equal to $N_0/2$.

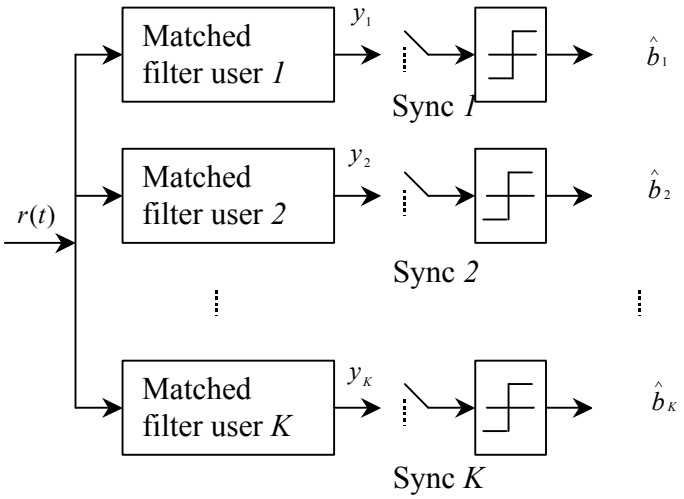

Figure 3.1 Conventional detector

The hard decision of the *k*th user is given by

$$\hat{b}_k = sign\{y_k\} \tag{3.8}$$

With a matrix-vector notation, it is convenient to express Eq. (3.6) as

$$\mathbf{y} = \mathbf{RAb} + \mathbf{n} \tag{3.9}$$

where $\mathbf{R}$ is the normalized crosscorrelation matrix given in Eq. (3.4)

$$\mathbf{y} = [y_1, \cdots, y_K]^T,$$

$$\mathbf{b} = [b_1, \cdots, b_K]^T,$$

$$\mathbf{A} = diag\{A_1, \cdots, A_K\},$$

and $\mathbf{n}$ is a zero mean Gaussian random vector with covariance matrix equal to

$$E[\mathbf{nn}^{\mathbf{T}}] = \frac{N_0}{2}\mathbf{I} \tag{3.10}$$

The second term on the right hand side (RHS) of Eq. (3.6) is the interference from other users (MAI). If the signature sequence of the *k*th user is orthogonal to the other signature waveforms, then $r_{k,j} = 0,\ j \neq k$. Thus the interference from the other users

vanishes and the conventional detector is optimum. On the other hand, if one or more of the other signature sequences are not orthogonal to the desired user's signature sequence, the interference from the other users can become excessive if the power levels of the signals (or the received signal energies) of one or more of the other users is sufficiently larger than the power level of the *k*th user. This is usually called the near-far problem in multiuser communications, and it necessitates some type of power control for conventional detection.

In asynchronous transmission, the conventional detector is more vulnerable to interference from other users. This is because there is no possibility of designing signature sequences for any pair of users that are orthogonal for all time offsets. Consequently, interference from other users is unavoidable in asynchronous transmission with the conventional detection. In such a case, the near-far problem resulting from unequal power in the signal transmitted by the various users is particularly serious. The practical solution is to incorporate power control or employ other multiuser detection strategies.

3.3.3 Optimum Detector (MLS Detector)

In [17], S. Verd? proposes a maximum likelihood sequence (MLS) multiuser receiver. The detector which yields the most likely transmitted sequence, $\mathbf{b}$, chooses $\mathbf{b}$ to maximize the probability that $\mathbf{b}$ was transmitted given that $r(t)$ was received [18]. This probability is referred to as the *joint a posteriori probability*, $P(\mathbf{b}|r(t))$ [15]. The performance advantages of MLS detection over conventional MF detection are huge: it yields tremendous BER improvements and capacity gains, and it solves the near-far problem.

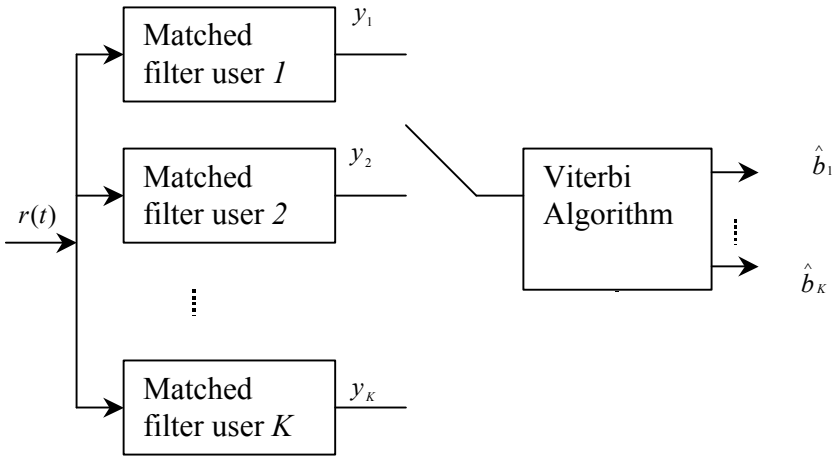

Figure 3.2 Optimum multiuser detector

Despite of these advantages, the exponential computational complexity of this detector makes the cost too high. Although the MLS detection can be implemented for DS-CDMA by following the matched filter bank with a Viterbi algorithm [19], the Viterbi algorithm has a complexity that is still exponential in the number of users, that is, on the order of 2^K. Therefore, it is impractical to implement in communication systems where the number of users is large.

Another problem with this detector is that it requires knowledge of the received amplitudes and phases. These values, however, are not known a priori; they must be estimated [18].

Due to the impractical property of the MLS detector, there is a need to design suboptimal detectors in order to reduce the receiver complexity. Most of the suboptimal detectors fall into two categories: linear detection and subtractive interference cancellations.

3.3.4 Linear Detector

The linear multiuser receiver is based on a set of appropriately chosen linear transformations on the outputs of a matched filter bank. It apply a linear mapping, $\mathbf{L}$,

to the soft output of the conventional detector to reduce the MAI seen by each user. The computation complexity of the linear detectors increases linearly with the number of users.

Decorrelating Detector

Since the conventional detector is vulnerable to the near-far problem, it requires some type of power control. The decorrelating detector is another type of detector that also has a linear computational complexity but does not exhibit the vulnerability to other-user interference. This kind of detector is not only a simple and natural strategy but it is optimal according to three different criteria: least-squares, near-far resistance, and maximum-likelihood when the received amplitudes are unknown [17].

The decorrelating detector applies the inverse of the correlation matrix

$$\mathbf{L}_{dec} = \mathbf{R}^{-1} \tag{3.11}$$

to the matched filter bank outputs, thereby decoupling the signals. The soft estimate of this detector is

$$\begin{aligned} \hat{\mathbf{d}} &= \mathbf{L}_{dec}\mathbf{y} \\ &= \mathbf{R}^{-1}\mathbf{y} \\ &= \mathbf{Ab} + \mathbf{R}^{-1}\mathbf{n} \end{aligned} \tag{3.12}$$

which is just the decoupled data plus a noise term. Thus, the MAI is completely eliminated. This detector is similar to the ZF equalizer [15] which is used to eliminate ISI.

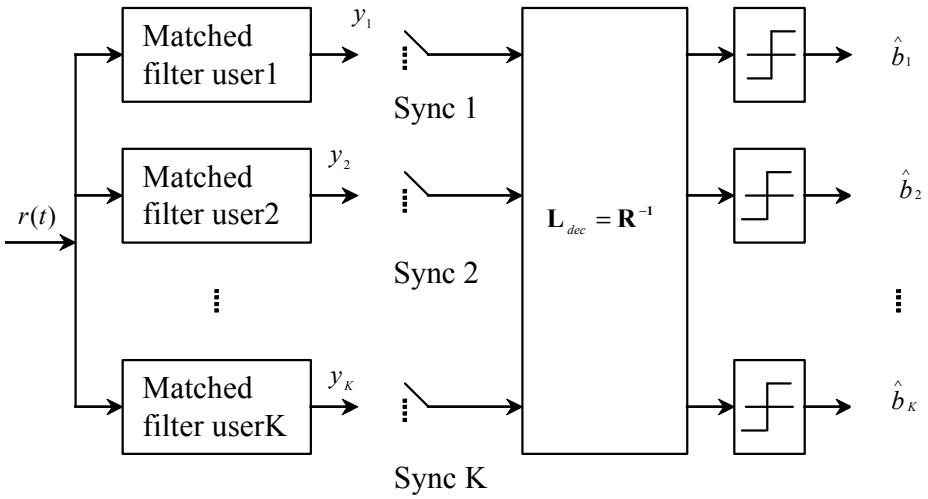

Figure 3.3 Decorrelating detector

From the implementation viewpoint, some desirable features of this multiuser detector are [17-18]:

- The computational complexity is significantly less than that of the optimal multi-user detector. The per-bit complexity is linear in the number of users, excluding the cost of re-computation of the inverse mapping.
- It does not require knowledge of the received amplitudes (the energies of the users).
- The near-far resistance is equal to that of the MLS detector.
- It corresponds to the maximum likelihood detector when the energies of all users are unknown at the receiver, i.e., it yields the joint maximum likelihood estimation of the amplitudes and the transmitted bits.
- The error rate per user is independent of the signal energies.
- Its performance analysis is fairly simple.

- One user can be decorrelated at a time. For user *k*, only the *k*th row of $\mathbf{L}_{dec} = \mathbf{R}^{-1}$ need to be applied to the matched filter bank outputs.

In decorrelating detection, the transformation eliminates the interference components. Consequently, the near-far problem is eliminated and there is no need for power control. But the transformation of $\mathbf{L}_{dec} = \mathbf{R}^{-1}$ does not include the noise component, so the decorrelating detection does not take into account the background noise, therefore one disadvantage of this detector is that it causes noise enhancement (similar to ZF equalizer), and if under the circumstances of sufficiently low signal-to-noise ratios, the conventional detector performs better than the decorrelating detector.

Minimum Mean-Squared Error (MMSE) Detector

The conventional detector is optimized to combat the background white noise exclusively, whereas the decorrelating detector eliminates the multiuser interference disregarding the background noise. In contrast, the MMSE linear detector can be seen as a compromise solution that takes into account the relative importance of each interfering user and the background noise. In fact both the conventional detector and the decorrelating detector are limiting cases of the MMSE linear detector.

MMSE detector implements the linear mapping which minimizes

$$e = E\left[\left|\mathbf{b} - \mathbf{L}_{\mathbf{MMSE}}\mathbf{y}\right|^2\right] \tag{3.13}$$

where $\mathbf{L}_{\mathbf{MMSE}}$ is the transformation matrix applied to the output of the matched filter bank to eliminate the MAI. The analysis in [17] gives the expression of $\mathbf{L}_{\mathbf{MMSE}}$ as

$$\mathbf{L}_{\mathbf{MMSE}} = \left(\mathbf{R} + \frac{N_0}{2}\mathbf{A}^{-2}\right)^{-1} \tag{3.14}$$

The format of the MMSE detector is very similar to that of the decorrelating detector, hence most of the suboptimum proposals mentioned earlier for the

decorrelating detector are applicable to this detector as well. As the background noise goes to zero, the MMSE detector converges to the decorrelating detector. However, the presence of noise will lead to a performance that depends on the interfering signal powers. Therefore, while the MMSE detector may yield improved performance in the presence of noise, there is some loss in its near-far resistance, as compare to the decorrelating detector.

3.3.5 Subtractive Interference Cancellation

The basic principle underlying these schemes is to create estimates at the receiver of the received signals of each individual user in order to subtract out some or all of the interfering signals (MAI) that each user sees. This approach is generally implemented in multiple stages. Tentative symbol decisions are formed at the output of one stage; these decisions are then used to regenerate and cancel out the MAI of each user in the next stage. The tentative symbol decisions can be hard decisions or soft decisions. Using soft decisions means that we simply use the outputs of the correlators as our symbol estimates. The hard-decision approach requires reliable estimates of the received powers and phases in order to regenerate good estimates of each user's signal. There is a strong similarity between this multiuser detection and the decision feedback equalization used in ISI channels; there, decisions on previously detected symbols are fed back in order to cancel part of the ISI.

There are two main varieties of such cancellation schemes: serial and parallel interference cancellation.

Serial Interference Cancellation (SIC)

This technique is often also referred to as successive interference cancellation. Each stage of this detector decides, regenerates, and cancels out one additional user from the

received signal, so that the remaining users see less MAI in the next stage. A simplified diagram of the first stage of this detector is shown in Figure 3.4. It implements the following steps [18]:

1. Detect the strongest signal, u_k with the conventional detector.
2. Make a hard data decision on u_k.
3. Regenerate an estimate of the received signal for user *k*, $u_k'(t)$, using
    a. Data decision from step 2
    b. Knowledge of its PN sequence
    c. Estimates of its timing, phase, and amplitude
4. Cancel $u_k'(t)$ from the total received signal, $r(t)$, yielding a modified received signal, $r_1(t)$.

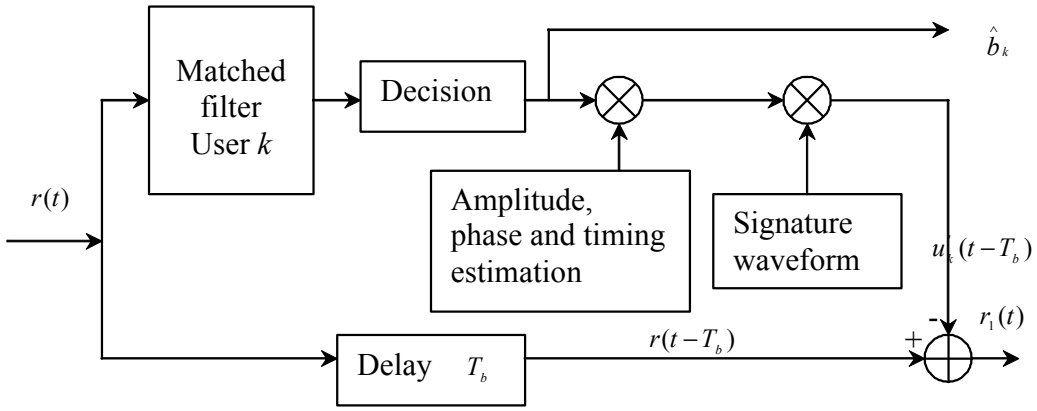

Figure 3.4 SIC detector – first stage

Assuming that the estimation in step 3 is successful, the outputs of the first stage are:

1. A correct data decision of the strongest user, $\hat{b}_k$.

2. A partially cleaned version of the received signal, $r_1(t)$, without the MAI due to the strongest user.

This process can be repeated in a multistage structure as shown in Figure 3.5; each successive stage takes as its input the modified received signal produced by the previous stage, and outputs one additional data decision and a supposedly "cleaner" received signal. The reasons for selecting signals for cancellation in descending order of signal strength are [16]: first, it is easiest to achieve acquisition and demodulation on the strongest users (best chance for a correct data decision). Second, the removal of the strongest users gives the most benefit for the remaining users. Note that the strongest user will not benefit from any MAI reduction; however, the weakest users will potentially see a huge reduction in their MAI.

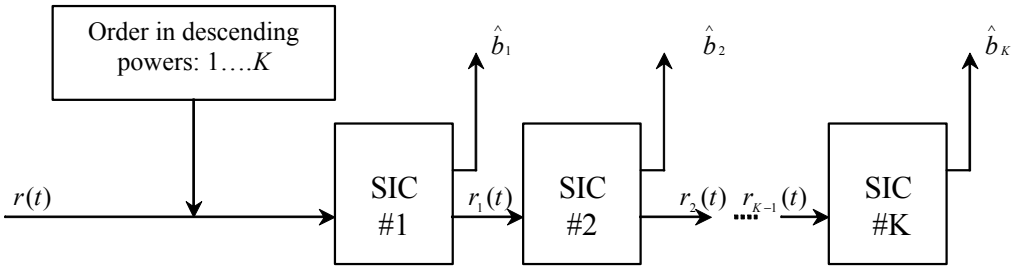

Figure 3.5 Multistage SIC detector

The success of this algorithm depends on successful data estimation. If the initial data decision or even the strongest users are unreliable, or if the timing, phase, and amplitude estimates are very poor, this technique breaks down; by subtracting a bad estimate, more noise is added than being canceled. While SIC only requires a minimum amount of additional hardware, it causes one additional symbol delay per

cancellation stage. How well this delay can be tolerated depends on the specific application.

Parallel Interference Cancellation (PIC)

An alternative to the SIC scheme is to take a parallel approach to the interference cancellation. In a PIC detector, symbol estimates from the output of the previous stage are used at each stage, to recreate and subtract out each user's MAI in parallel. The first stage of such a detector is pictured in Figure 3.6. Note that the partial summer sums up all but one signal at each of the *K* outputs, thus creating MAI estimates for each user. The inputs to this stage are tentative data estimates that are derived from the MF outputs.

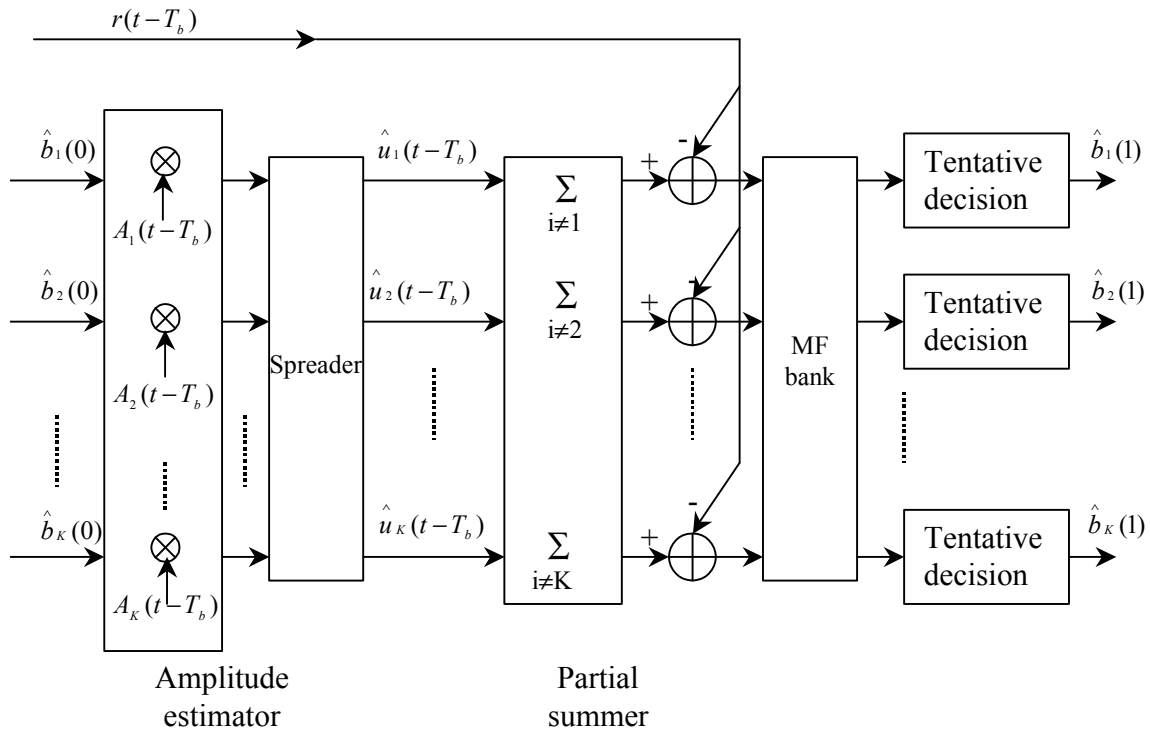

Figure 3.6 One stage of PIC detector

If the initial data estimate is correct, perfect cancellation of the signal can be achieved; if, however, it is incorrect, the noise component will be doubled due to this

interfering signal. The potential gains from this technique thus depend significantly on the initial tentative data estimates. Therefore, the matched filter bank in Figure 3.6 may be replaced by the decorrelating detector, which yields better initial tentative decisions. Another benefit from this hybrid detector is that the performance analysis is found to be much simplified.

The PIC process can then be repeated in a second stage, using the outputs of the first stage as the data inputs. In this way a new set of better data estimates will be generated at the outputs of stage 2. A block diagram of a multistage detector is pictured in Figure 3.7.

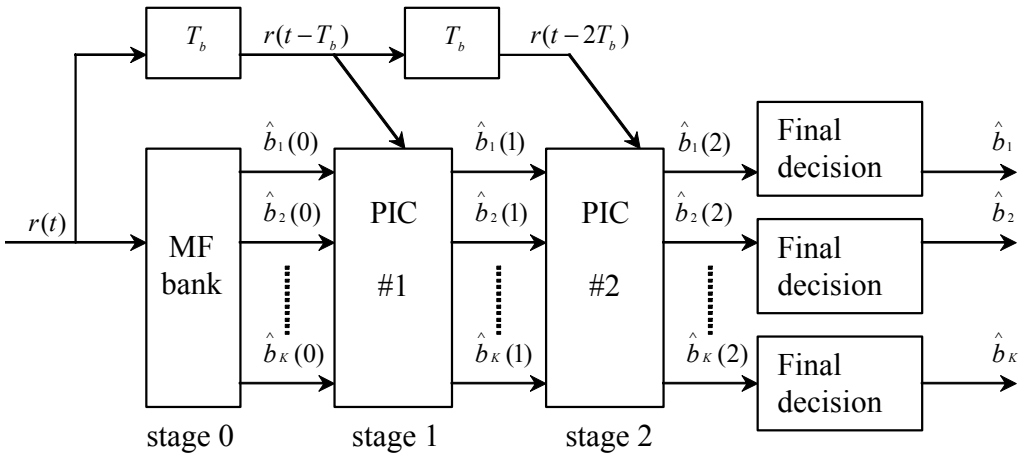

Figure 3.7 Multistage PIC detector, two stages are shown

In PIC detection, performance may be enhanced when multistage is introduced. Yet one problem with multistage PIC is that it cannot guarantee a performance improvement with more stages. For example, when a wrong estimation of the received signal is applied, degradation is introduced.

In view of the disadvantages associated with the conventional multistage PIC, D. Divsalar *et al*. [20] suggested a partial cancellation of the MAI at each stage. The

amount of the IC is decided by a weighting factor at each stage for all users. When the weight is properly chosen, this method can ensure a better performance after the partial interference cancellation. Since the estimates of the users' data become more reliable when more MAI has been cancelled, they propose to increase the weighting factor for each successive stage.

3.4 Summary and Comparison of the Multiuser Detection Schemes

Conventional DS-CDMA systems are limited by multiple access interference, or MAI. *The conventional detector* consists of a bank of matched filters, with each filter matched to a particular user's code waveforms; thus each user is detected in a separate receiver branch without regard for the other users (a bank of single-user detectors). In multiuser detection, code and timing information of multiple users are jointly used to better detect each individual user.

The MLS detector yields optimum performance, but it is too complex to implement for practical systems. It consists of a bank of matched filters followed by a Viterbi algorithm, with complexity that is exponential in the number of users. The Viterbi algorithm can be simplified with suboptimal sequential decoding techniques, but these too, are fairly complex to implement.

Linear multiuser detectors, which include the decorrelating detector and the minimum mean-squared error (MMSE) detector, apply a linear mapping to the outputs of the matched filter bank, so as to reduce the MAI that each user sees.

The decorrelating detector applies the inverse of the correlation matrix to the matched filter bank outputs, thereby decoupling the signals. It has many desirable features including an ability to be implemented without knowledge of the received amplitudes. A disadvantage of this detector is that it causes noise enhancement. The

power associated with the noise term at the output of the decorrelating detector is always greater than or equal to the power associated with the noise term at the output of the conventional detector for each bit. A more significant disadvantage of the decorrelating detector is that the computations needed to invert the crosscorrelation matrix are difficult to perform in real time [18].

The MMSE detector applies a modified inverse of the correlation matrix to the matched filter bank outputs. It balances the desire to decouple the users (and completely eliminate MAI) with the desire to not enhance the background noise. This detector is exactly analogous to the MMSE linear equalizer used to combat ISI. Because it takes the background noise into account, the MMSE detector generally provides better performance than the decorrelating detector. An important disadvantage of this detector is that, unlike the decorrelating detector, it requires estimation of the received amplitudes. Another disadvantage is that its performance depends on the powers of the interfering users. Therefore, there is some loss of resistance to the near-far problem as compared to the decorrelating detector. Like the decorrelating detector, the MMSE detector faces the task of implementing the matrix inversion [18].

In contrast to linear detector, the subtractive interference cancellation (IC) attempts to regenerate and subtract off the MAI. This type of detector may consist of either single or multiple stages. A major disadvantage of nonlinear detectors is their dependence on reliable estimates of the received amplitudes. Imperfect amplitude estimation may significantly reduce or even reverse the gains that can otherwise be obtained from using these detectors. Two of the most cited subtractive interference cancellation techniques are *successive interference cancellation* (SIC) and *parallel interference cancellation* (PIC).

The advantage of ***the SIC detector*** is that it requires only a minimum amount of additional complexity. However, canceling one user in SIC will cause one bit delay. When the number of users is large, the excessive delay will become unacceptable. In general, PIC will cause much less delay as compared to SIC. Yet its complexity is higher than SIC.

In [21], the performance of an SIC scheme is compared with the standard multistage PIC detector for asynchronous DS-CDMA system with BPSK modulation and coherent detection. In the SIC approach, the cancellation is conducted in an order from the strongest to the weakest according to the users' power levels. Under imperfect power control, SIC scheme is superior to PIC. However, with perfect power control, PIC shows greater capacity tolerance than SIC.

A conclusion is reached in [22] which declared that the multistage PIC is the most promising multiuser detection technique for the DS-CDMA system. The detailed description of the advantages and disadvantages of PIC versus SIC in [22] are presented below:

The first advantage of PIC over SIC is that the former does not need any user ranking. For SIC, the ranking can be based on the instantaneous output of each user's matched filter or on an average power estimate.

Another drawback of SIC, as mentioned previously, is the demodulation delay experienced by the weaker users in the first stage and for all users, if more than one stage is employed. Another drawback of the SIC is the re-ordering of users every time their ranking changes. This complicates the implementation (e.g. a pipelined structure for the SIC).

For SIC, the advantage of having users with substantially different powers is diminished because of fast power control. Nevertheless, users in soft handoff have

their power controlled by one of the base stations and are therefore received at the remaining base stations with different power than other signals. At those base stations, the performance of the users in soft handoff will be better with SIC. Also, when some of the users experience imperfect power control and/or fast fading, the corresponding received powers will be sufficiently different and make the SIC preferable.

When conventional SIC is implemented, the matched filters of *K-1* users are inactive when a decision and respreading are performed for one user each time. This has the advantage of reduced computational complexity in MIPS (Million-Instruction-Per-Second) at the expense of longer delay. However, the increased MIPS required by the PIC seem to be the only complexity drawback of that method relative to SIC.

Chapter 4

APIC Receiver for Synchronous MC-DS-CDMA System

4.1 Motivation

Transmission over frequency selective multipath fading is common in the wireless communication environments and is a main impairment resulting in the degradation of a wideband mobile communication system. As we have mentioned, since conventional single carrier (SC) DS-CDMA systems are broadband when used for high data rate applications, multipath propagation causes ICI and severe ISI if the channel delay spread exceeds the symbol duration, in other words, the bandwidth of the SC-DS-CDMA system is wider than the coherent bandwidth of the channel. Under these effects, if no coding or diversity is implemented, the performance of the SC-DS-CDMA system degrades rapidly when the number of users increases [23]. On the other hand, frequency selective fading provides the opportunity for diversity inherent in multipath propagation and a RAKE receiver [15], [24] can be utilized to take advantage of this opportunity and thus enhance system performance.

The ideal RAKE receiver has as many correlator arms (or called "fingers") as the resolvable paths. The practical RAKE receiver, however, has much fewer arms than the ideal one. A SC RAKE receiver capable of tracking L resolvable paths will recover less and less power from paths having longer delays. However, if the bandwidth used by the SC RAKE system is divided into several subbands such as M subbands, then the

number of resolvable paths within each subband is less, but more power can be recovered from each path. Restricting the range of frequencies, we get less frequency selective fading within each subband and more energy can be recovered. Alternatively, from a time domain perspective, delays between paths carrying signals within a small frequency range, are smaller and a RAKE receiver can capture more of these paths. This way the received energy is maximized. Considering the extreme case where the bandwidth of a subband is chosen equal to the coherent bandwidth of the channel, then each subband experiences flat fading only, similar to OFDM. In this case, all the energy can be recovered from a single resolvable path. That is the benefit we can get from the MC systems. In addition, a MC system requires a lower speed, parallel-type of signal processing, in contrast to a fast, serial-type of signal processing in a SC RAKE system. This might be helpful for use with a low power consumption device [25].

In chapter 2, various types of MC CDMA systems have been compared. As we have seen, all these systems have similar fading mitigation effect over a frequency selective channel. However, the MC-DS-CDMA system needs fewer carriers and thus allows the processing gain (PG) to be increased. It also simplifies the receiver because it requires fewer amplifiers in the diversity combiner. This system was originally proposed for an uplink communication channel because the introduction of OFDM signaling into DS-CDMA system is effective for the establishment of a quasi-synchronous channel [12]. Hence it is desirable for uplink transmission because it does not require the users to be synchronized. With all these advantages, to improve the system performance of the MC-DS-CDMA system has become the target of this thesis.

As mentioned before, although MC-DS-CDMA system is a promising candidate for both high bit rate data transmission and high system capacity, the MAI problems

inherent to the SC-DS-CDMA system also limit the performance of the MC-DS-CDMA system. The issue of signal detection for the MC-DS-CDMA system is the same with that for SC-DS-CDMA. Detectors for MC-DS-CDMA can also be grouped into two basic categories: Single-user detectors and multiuser detectors. In the first category, the receiver has knowledge of the spreading sequence employed by the user of interest only, which means that it has no knowledge of the spreading sequence employed by other users. Interference from other users is assimilated to additive channel noise and no attempt is made to compensate for it. In the second category, the receiver has knowledge of spreading sequence employed by other users and exploits this knowledge for signal detection. In multiuser detectors based on interference cancellation (IC), the interference affecting each user is explicitly synthesized and subtracted from the received signal before sending it to a threshold detector.

In some research literatures [6], [25], [26], the single-user detection strategy is used for MC-DS-CDMA system. One of the multiuser detection algorithms, the SIC, was adopted in [27] and the comparison was made between SIC, MMSE and MF receiver with MRC. In this thesis, another multiuser detection algorithm – PIC detection is used as the detection strategy. As has been mentioned in Chapter 3, the PIC detector is one of the promising nonlinear suboptimal detectors [28]. Yet the potential gain from applying this technique depends significantly on the quality of MAI estimates. An improved PIC detector was proposed in [20], where partial MAI cancellations are used to mitigate the effect of unreliable estimations. Motivated by [20], a multistage PIC with adaptive MAI cancellation in the SC-DS-CDMA system was proposed in [29]. In this chapter, such an adaptive PIC (APIC) technique together with the maximal ratio combing (MRC) is adopted in the synchronous MC-DS-CDMA system.

Investigation has shown that by using MRC before and after the APIC receiver in order to exploit the diversity provided by the MC-DS-CDMA system, significant performance improvement can be achieved over the MF receiver and the conventional PIC (CPIC) receiver.

4.2 Diversity Combining Techniques

In a single-user setting, MC CDMA systems can exploit all the available frequency diversity by employing combining techniques such as MRC. In a multiuser setting, however, the capacity of the single-user MRC detector is limited by multiuser interference. There has been great interest in improving the MC CDMA detection by amalgamating the multiuser detection and the combining techniques. Since diversity combining techniques are crucial to MC CDMA systems, a brief introduction of the variety of such techniques may be helpful before describing the system model of the proposed APIC receiver.

In a broad sense, there are three major generic diversity signal-processing techniques, and they are known as *selection diversity* (SD), *equal gain combining* (EGC), and *maximal ratio combining* (MRC) [7].

4.2.1 Selection Diversity (SD)

Consider an L-fold diversity transmission system. Regardless of the type of diversity, there must be L receivers in the sense that each of the L transmissions must be received separately. In this system, the signal diversity component received with the highest SNR is chosen for signal demodulation, and the remaining $L-1$ components are ignored. Figure 4.1 depicts a selection diversity reception scheme for an L-fold diversity transmission system.

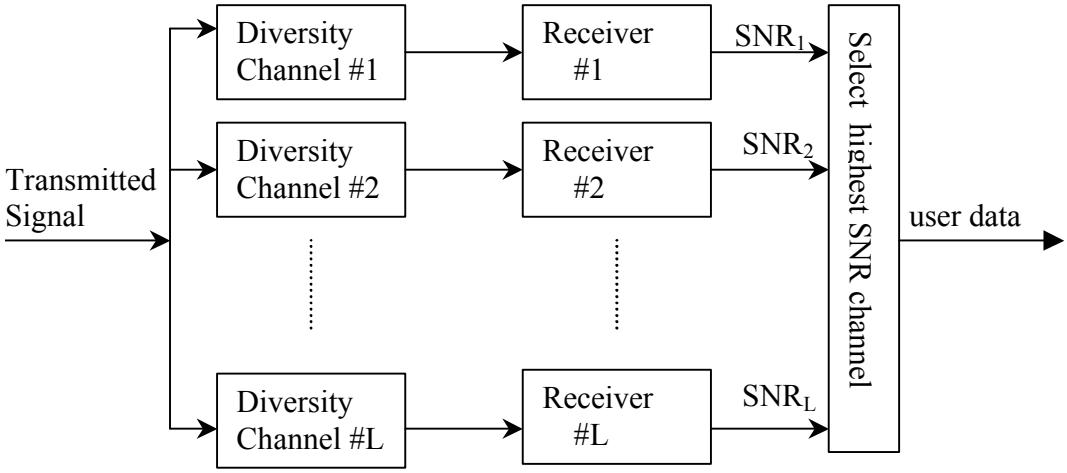

Figure 4.1 postdetection selection-diversity receiver model

4.2.2 Equal gain combining (EGC)

Different from *selection diversity,* the symbol decision statistics of *equal gain combining* technique for each branch are combined (summed) with equal gains to obtain the overall decision statistics. Figure 4.2 is a postdetection EGC receiver with the fact that, for equal gain combining and independent noise in each diversity channel, the SNR at the output of the combiner is the sum of the channel SNRs.

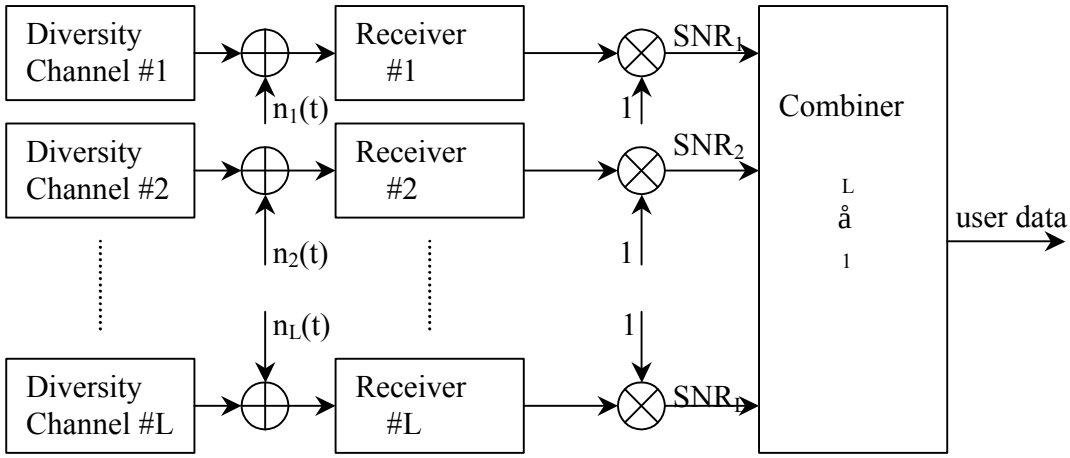

Figure 4.2 postdetection EGC receiver model

4.2.3 Maximal ratio combining (MRC)

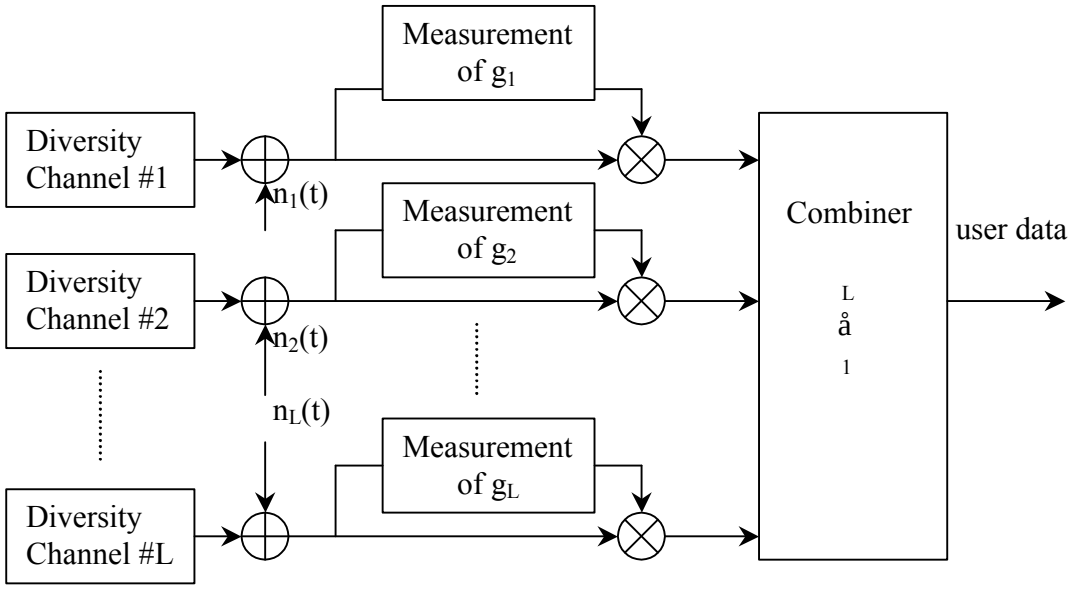

Figure 4.3 Complex envelope diagram of MRC diversity reception

In *maximal ratio combining (MRC)* diversity reception, the phases of the diversity signals being added together are aligned (made mutually coherent) and their envelopes are weighted in proportion to the square roots of the diversity SNRs. MRC is the optimal form of diversity combining because it yields the maximal SNR achievable. The optimal combining requires exact knowledge of the SNRs as well as the phases of the diversity signals. And it achieves an SNR at the combiner output that is equal to the sum of the SNRs in the diversity channels. Basically, MRC is similar to EGC, except that each diversity channel is multiplied, not by an "equal gain," but by a gain proportion to the square root of the SNR of the channel. Therefore, the performance of EGC diversity reception behaves in a way that is similar to that of MRC and yields a lower bound, because MRC is the optimal form of combining.

The principle of MRC reception is that we multiply the received waveform by the gain g_n, which is complex in general, and then add the output of the diversity channels

as indicated in Figure 4.3. The objective is to find the specific form of g_n to be proportion to the square root of SNR_n, the channel SNR.

4.3 System Model

In this chapter, the synchronous system is investigated. The reason for studying the synchronous system is that it considerably simplifies the exposition and analysis and often permits the derivation of closed-form expressions for the desired performance measures. They are useful since similar trends are found in the analysis of the more complex asynchronous case. Furthermore, every asynchronous system can be viewed as an equivalent synchronous system with larger effective user population [35], which is often explored in burst CDMA communications. Moreover, synchronous systems are becoming more of practical interest since quasi-synchronous approach has been proposed for satellite and microcell applications [36]. Since the MC-DS-CDMA system is originally proposed for quasi-synchronous channel, it is valuable to study the synchronous case first.

4.3.1 Transmitter

In the MC-DS-CDMA system, the available frequency spectrum is split into a number of smaller frequency bands. Each band is used to transmit a narrowband direct sequence waveform. The structure of the transmitter for user *k* is shown in Figure 4.4. The transmitting bit stream with duration $T_b^{'}$ is converted into *P parallel-bit* branches. The new bit duration $T_b = PT_b^{'}$ on each branch can suppress ISI. Each parallel branch data is then copied into *M* streams defined as *identical-bit* streams to achieve frequency diversity and suppress ICI. These $M \times P$ identical-bit streams are all spread by the same pseudo random spreading sequences that uniquely identify each user in the

system. Each stream is then assigned a carrier that is orthogonal to each other. The $M \times P$ frequencies are assigned such that given a value P, the frequency separation between two successive identical-bit carriers is maximized, as shown in Figure 4.5. We adopt the carrier assignment that allows the frequency spectrum of each carrier to overlap such that we can achieve better spectral efficiency. In general, multicarrier schemes should use OFDM signaling for the sake of efficient frequency spectrum utilization because OFDM can minimize the guard frequency space between adjacent subcarriers [5]. Meanwhile, the OFDM signaling can be efficiently implemented by using fast Fourier transform technique, which can be easily realized with current digital signal processing (DSP) chips.

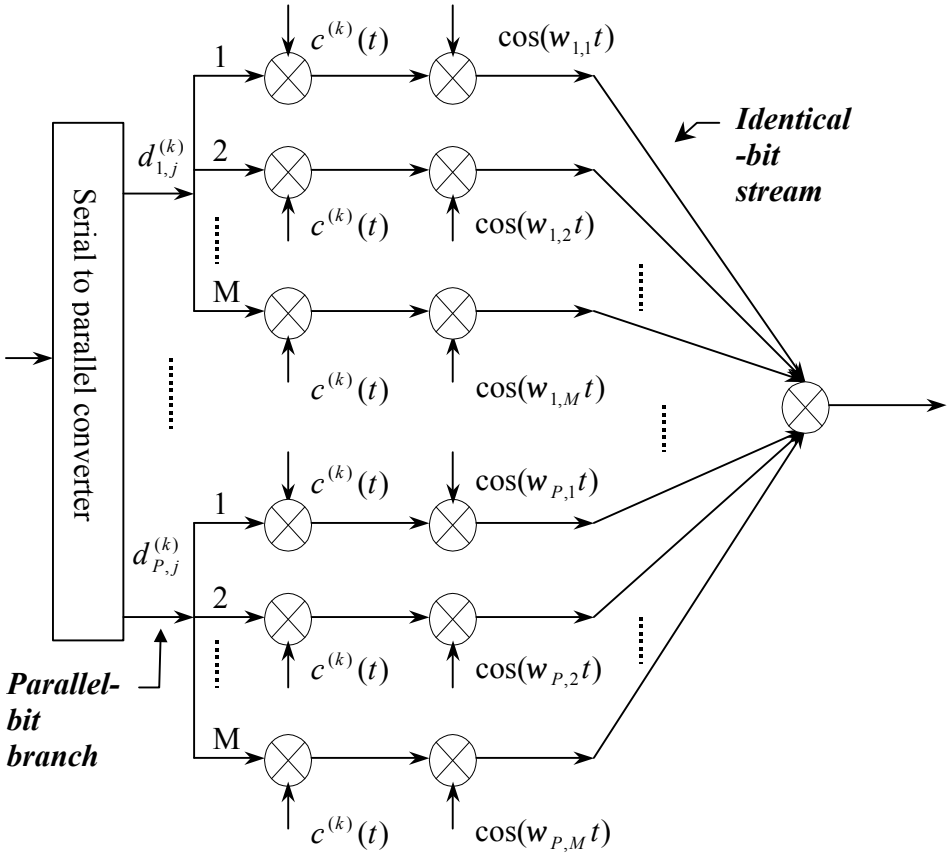

Figure 4.4 Transmitter of MC-DS-CDMA

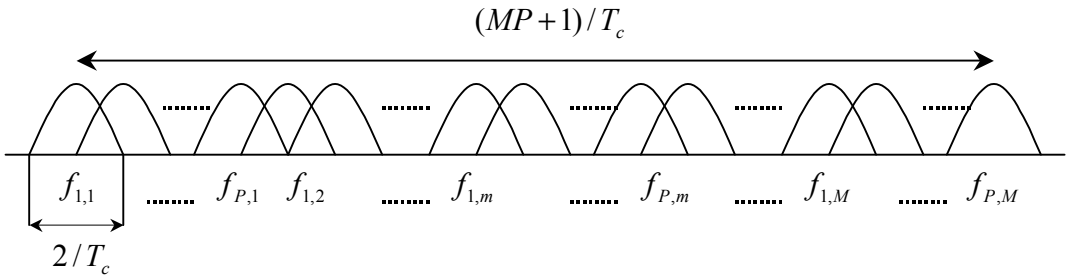

Figure 4.5 Frequency spectrum of the signal

4.3.2 Channel

The channel is assumed to be a slowly varying, frequency selective Rayleigh fading channel with delay spread T_m. Since the spread spectrum system can resolve multipath signals with delay larger than one-chip duration, for SC-DS-CDMA system, the complex lowpass equivalent impulse response of the channel can be modeled as

$$h(t) = \sum_{l=0}^{L'-1} z_l' d\left(t - lT_c'\right) \tag{4.1}$$

where T_c' is the chip duration of the SC-DS-CDMA system and z_l' is the channel gain of the $(l+1)$th path and it is a zero mean, complex Gaussian r.v.. L' is the number of the multipath and is determined by

$$L' = \lfloor T_m / T_c' \rfloor + 1 \tag{4.2}$$

Assuming a passband null-to-null bandwidth, the transmission bandwidth for the SC-DS-CDMA system is $2/T_c'$. If we denote the chip duration on each subcarrier of the MC-DS-CDMA system as T_c, to keep the bandwidth fixed, the following condition should be satisfied (see Figure 4.5):

$$\frac{2}{T_c'} = (PM+1)\frac{1}{T_c} \tag{4.3}$$

For comparison purpose, we present the relationship of the processing gain of the SC- DS-CDMA and MC-DS-CDMA systems, i.e., N' and N respectively. To keep the bandwidth constant, they must follow [6]:

$$N = \frac{2P}{PM+1} N' \tag{4.4}$$

The objective of multicarrier systems is to make the frequency selective fading channel appear as flat fading on each subcarrier. To fulfill this goal, the channel should be a single-fading channel for each subcarrier. From Eq. (4.2) and Eq. (4.3), the number of resolvable paths for each subcarrier is $L = \lfloor T_m / T_c \rfloor + 1 = \lfloor 2(L'-1)/(MP+1) \rfloor + 1$. In order to make $L = 1$, P and M should satisfy

$$MP \geq 2(L'-1) \tag{4.5}$$

If the number of P and M properly selected, each subcarrier experiences a flat-fading channel. The complex channel gain for the qth subcarrier of user k is denoted as

$$z_q^{(k)}(t) = a_q^{(k)}(t) \exp\left[j b_q^{(k)}(t) \right] \tag{4.6}$$

where $a_q^{(k)}(t)$ is a Rayleigh-distributed stochastic process with unit second moment while $b_q^{(k)}(t)$ is uniformly distributed over 0 and $2p$. It is assumed that $z_q^{(k)}(t)$ is i.i.d. for different k and q. This is a slight simplification over a real channel which would be correlated in frequency, but typically the difference in performance for correlated modeling is small [27], [30].

In this chapter, a synchronous MC-DS-CDMA system of K users with BPSK modulation on each subcarrier is considered. The received signal is given by

$$r(t) = \sum_{k=1}^{K} \sum_{j=-\infty}^{\infty} \sum_{p=1}^{P} \sum_{m=1}^{M} \sqrt{\frac{2P_k}{M}} d_{p,j}^{(k)} p_{T_b}(t - jT_b) c^{(k)}(t) z_q^{(k)} \cos(w_q t) + n(t) \quad , \tag{4.7}$$

where P_k is the power of the kth user, $d_{p,j}^{(k)}$ is the jth bit of the kth user's pth parallel-

bit data, taking the value of ± 1. $p_t(t)$ is defined as the rectangular pulse waveform with unit amplitude and duration t . w_q is the qth carrier frequency and $c^{(k)}(t)$ is the spreading sequence of user k, which is given by

$$c^{(k)}(t) = \sum_{n=-\infty}^{\infty} c^{(k)}(n) p_{T_c}(t - nT_c) \tag{4.8}$$

where $c^{(k)}(n)$ is the nth chip of the spreading sequence of user k. The spreading sequence is normalized such that $\sum_{n=0}^{N-1}\left[c^{(k)}(n)\right]^2 = 1$, where N is the processing gain (PG). Note that we have assumed the channel is fading slowly such that the channel gain $z_q^{(k)}$ remains constant for one-bit duration. Hence instead of denoting it as function of time, we introduce a subscript j so that now $z_{q,j}^{(k)} = a_{q,j}^{(k)} \exp\left[jb_{q,j}^{(k)}\right]$ represents the channel gain at the jth symbol. The parameter $q = p + (m-1)P$ is the carrier number index corresponding to the pth parallel branch and the mth identical-bit stream. Lastly, $n(t)$ is the additive white gaussian noise (AWGN) with zero mean and one-sided power spectral density of N_0.

4.4 Receiver Structure

4.4.1 Initial Stage: MF with MRC (MF-MRC)

Referring to Figure 4.6, after the received signal is down converted to its equivalent baseband signal and passed through the FFT block, the signal can be grouped into P sets, each comprising of the M identical-bit streams. For simplicity, only the pth branch will be considered in the following description. Without loss of generality, let us examine the detection of the *0*th bit ($j = 0$). At the qth carrier, the coherently detected signal corresponding to the nth chip, denoted here as $r_q(n)$, where $q = p + (m-1)P$, is

given by

$$r_q(n) = \int_{nT_c}^{(n+1)T_c} r(t)\cos(w_q t)dt$$

$$= \sum_{k=1}^{K} v_q^{(k)}(n) + h_t(n),\ 0 \le n \le N-1 \tag{4.9}$$

where

$$v_q^{(k)}(n) = \sqrt{\frac{P_k}{2M}} d_{p,0}^{(k)} c^{(k)}(n) z_{q,0}^{(k)} \tag{4.10}$$

$$h_t(n) = \int_{nT_c}^{(n+1)T_c} n(t)\cos(w_q t)dt \tag{4.11}$$

h_t being a zero mean Gaussian r.v. with variance $s_h^2 = N_0/2$.

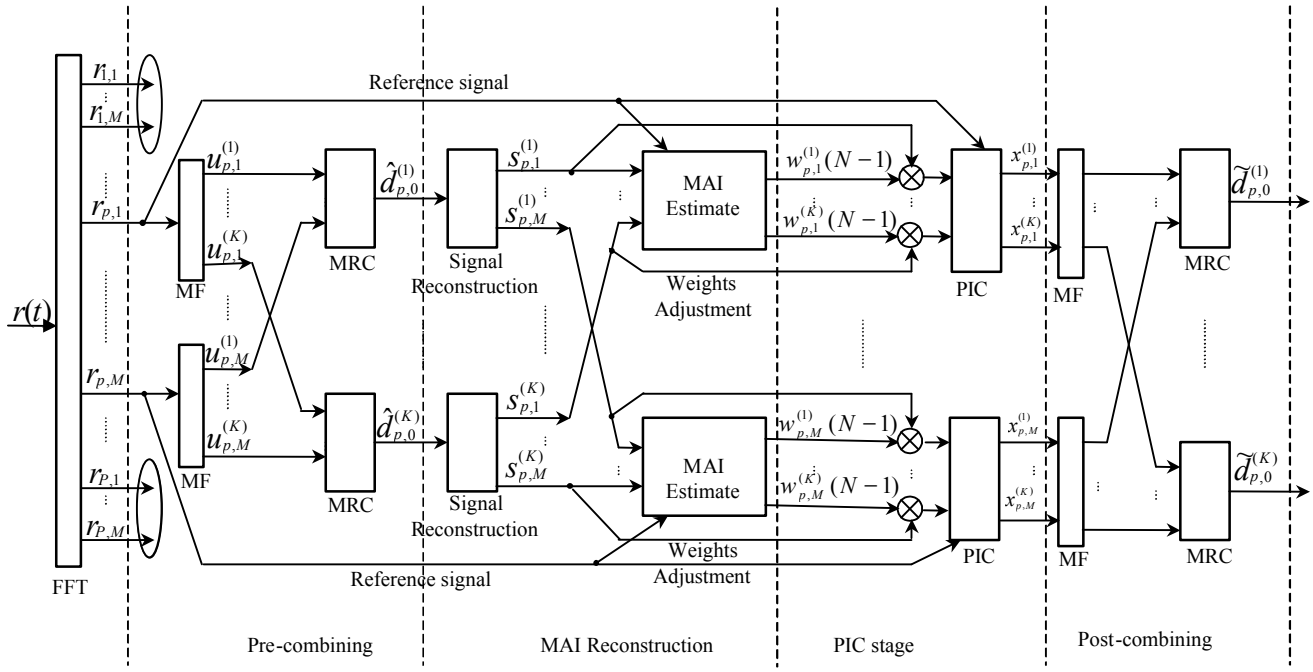

Figure 4.6 Receiver structure for synchronous MC-DS-CDMA

This signal $r_q(n)$ is passed to the chip-rate MF bank and the output corresponding to the *n*th chip of the *k*th user is given by

$$u_q^{(k)}(n) = r_q(n)c^{(k)}(n), \quad 0 \le n \le N-1 \tag{4.12}$$

The M outputs corresponding to the same user are then combined together using the MRC coefficients $g_{q,0}^{(k)} = \left[z_{q,0}^{(k)}\right]^*$, assuming perfect channel estimation, where $[x]^*$ is the complex conjugate of x. Tentative decisions regarding the transmitted bits are then made after the MRC. If the user of interest is user one, then the initial decision is given by

$$\hat{d}_{p,0}^{(1)} = sign\left\{\Re\left[\sum_{n=0}^{N-1}\sum_{m=1}^{M} u_q^{(1)}(n) g_{q,0}^{(1)}\right]\right\} \tag{4.13}$$

This is the output of the MF with MRC combining, which constitutes the initial stage of the receiver structure, as shown in Figure. 4.6.

4.4.2 MAI Estimation Stage

To reconstruct the MAI, M copies of the initial decision $\hat{d}_{p,0}^{(k)}$ of Eq. (4.13) are created, as shown in Figure 4.6. Similar to the transmitter, each of the M copies is spread by the corresponding user's spreading code $c^{(k)}(n)$ and attenuated by the channel gain $z_{q,0}^{(k)}$. Hence the regenerated signal of the nth chip corresponding to the qth carrier is given by

$$s_q^{(k)}(n) = \sqrt{\frac{P_k}{2M}}\hat{d}_{p,0}^{(k)} c^{(k)}(n) z_{q,0}^{(k)}, 1 \le m \le M \tag{4.14}$$

The regenerated signals of all the users are multiplied by the adaptive weights $w_q^{(k)}(n)$ and then summed together to produce an estimation of chip signal $r_q(n)$, i.e.,

$$\hat{r}_q(n) = \sum_{k=1}^{K} s_q^{(k)}(n) w_q^{(k)}(n), 0 \le n \le N-1 \tag{4.15}$$

Similar to [29], we define the cost function of our adaptive algorithm as the mean-squared value of the estimation error for the mth diversity branch. Hence,

$$e_q = E[|e_q(n)|^2] \tag{4.16}$$

where $E[\cdot]$ denotes the statistical expectation operator and $e_q(n) = r_q(n) - \hat{r}_q(n)$ is the estimation error. To minimize Eq. (4.16), the weights $w_q^{(k)}(n)$ are adjusted based on the normalized least-mean-square (LMS) algorithm [31] that operates over a bit interval and on a chip basis according to

$$w_q^{(k)}(n+1) = w_q^{(k)}(n) + \frac{m \cdot s_q^{(k)}(n)}{\sum_{k=1}^{K}[s_q^{(k)}(n)]^2}[e_q(n)]^* \tag{4.17}$$

where m denotes the step-size. Hence the number of iterations is equal to the PG, since the weights are adjusted at the chip rate over a one-bit interval. At the end of the iteration, the final weight $w_q^{(k)}(N-1)$ is obtained, which will be used by the next stage of the receiver, as described below. Note that for the CPIC receiver, there is no adaptive process involved. Hence this is equivalent to setting $w_q^{(k)}(N-1) = 1$.

4.4.3 Cancellation with MRC Stage: PIC-MRC

At the interference cancellation step, the weight $w_q^{(k)}(N-1)$ will be used to multiply the input signal $s_q^{(k)}(n)$ over the entire bit interval. Hence the interference cancellation for user one is performed as

$$x_q^{(1)}(n) = r_q(n) - \sum_{k=2}^{K} \hat{v}_q^{(k)}(n). \tag{4.18}$$

where

$$\hat{v}_q^{(k)}(n) = s_q^{(k)}(n) w_q^{(k)}(N-1) \tag{4.19}$$

The composite signal $x_q^{(1)}(n)$ is then passed into the MF bank where the M diversity identical-bit streams are combined via MRC. Final decisions are then obtained according to

$$\tilde{d}_{p,0}^{(1)} = sign\left\{\Re\left[\sum_{n=0}^{N-1}\sum_{m=1}^{M} x_q^{(1)}(n)c^{(1)}(n)g_{q,0}^{(1)}\right]\right\} \tag{4.20}$$

The multi-stage APIC receiver can be realized by repeating Eq. (4.14) to Eq. (4.20).

In Figure 4.6, if the final decisions are taken after the initial stage, then the structure becomes the MF with MRC combining, which we will refer to as the MF-MRC receiver. However if we consider the entire receiver structure but set the weight $w_q^{(k)}(N-1)=1$ in the MAI estimation stage, then the receiver becomes the CPIC receiver. For comparison purpose, we will present the performance analysis of the MF-MRC receiver, the CPIC receiver and the APIC receiver in the next section.

4.5 Performance Analysis

4.5.1 Analysis of MF-MRC Receiver

The soft output of the MF-MRC receiver of user one is given by

$$\begin{aligned} Z^{(1)} &= \Re\left\{\sum_{m=1}^{M}\sum_{n=0}^{N-1} u_q^{(1)}(n)\left[z_q^{(1)}\right]^*\right\} \\ &= D + n_t + I_{MAI} \end{aligned} \tag{4.21}$$

where $u_q^{(1)}(n)$ was defined in Eq. (4.12). The desired signal D can be written as

$$\begin{aligned} D &= \sum_{m=1}^{M}\sum_{n=0}^{N-1} v_q^{(1)}(n)c^{(1)}(n)\left[z_{q,0}^{(1)}\right]^* \\ &= \sum_{m=1}^{M}\sum_{n=0}^{N-1}\sqrt{\frac{P_k}{2M}}d_{p,0}^{(1)}\left[c^{(1)}(n)\right]^2\left|z_q^{(1)}\right|^2 \end{aligned}$$

$$= \sqrt{\frac{P_1}{2M}} d_{p,0}^{(1)} \sum_{m=1}^{M} \left[a_q^{(1)} \right]^2 \tag{4.22}$$

The noise term n_t is given by

$$n_t = \Re\left\{ \sum_{m=1}^{M} \sum_{n=0}^{N-1} h_t(n) c^{(1)}(n) a_{q,0}^{(1)} \exp\left[- j b_{q,0}^{(1)} \right] \right\} \tag{4.23}$$

with zero mean and variance given by

$$s_n^2 = \frac{N_0}{4} \sum_{m=1}^{M} \left[a_q^{(1)} \right]^2 . \tag{4.24}$$

The term I_{MAI} in Eq. (4.21) is the MAI, which can be written in two parts:

$$I_{MAI} = I_{MAI}^{(s)} + I_{MAI}^{(d)} \tag{4.25}$$

where $I_{MAI}^{(d)}$ is the interference from the other users on different carriers. Since only the synchronous case is studied, we can easily find that $I_{MAI}^{(d)}$ equals to zero. The other term $I_{MAI}^{(s)}$ refers to the interference from the other users on the same carrier, which is given by

$$I_{MAI}^{(s)} = \Re[\sum_{m=1}^{M} \int_0^{T_b} \sum_{k=2}^{K} \sum_{j=-\infty}^{\infty} \sqrt{\frac{2P_k}{M}} d_{p,j}^{(k)} p_{T_b}(t - jT_b) c^{(k)}(t) z_{q,0}^{(k)} \cos(w_q t) \cdot c^{(1)}(t) \cos(w_q t) \left[z_{q,0}^{(1)} \right]^* dt \ ]$$

$$= \sum_{m=1}^{M} \sum_{k=2}^{K} \sum_{n=0}^{N-1} \sqrt{\frac{P_k}{2M}} d_{p,0}^{(k)} c^{(k)}(n) c^{(1)}(n) \cdot \cos(b_{q,0}^{(k)} - b_{q,0}^{(1)}) a_{q,0}^{(k)} a_{q,0}^{(1)} \tag{4.26}$$

The term $I_{MAI}^{(s)}$ can be approximated as a zero mean Gaussian r.v. with a variance given by

$$Var\left[I_{MAI}^{(s)} \right] = \sum_{k=2}^{K} \frac{P_k}{4MN} \sum_{m=1}^{M} \left[a_q^{(1)} \right]^2 \tag{4.27}$$

Assuming that $E\left[\left(a_{q,0}^{(k)} \right)^2 \right] = 1$. If we let $g = \sum_{m=1}^{M} \left[a_{q,0}^{(1)} \right]^2$, and assume that a bit '1' is transmitted, then the BER conditioned on g is given by

$$P[e|g] = \frac{1}{2} erfc\left(\frac{E[Z^{(1)}]}{\sqrt{2Var[Z^{(1)}]}} \right)$$

$$= \frac{1}{2} erfc\left(\frac{\sqrt{\frac{P_1}{2M}} g}{\sqrt{2\left(Var[I_{MAI}] + s_n^2\right)}} \right) \tag{4.28}$$

Assuming that any bit can be sent via any of the P parallel branches with equal probability, the final BER can be written as

$$P_{ini}[e] = \frac{1}{P} \sum_{p=1}^{P} \int_0^{\infty} P[e|g] p(g) dg \tag{4.29}$$

where $p(g)$ is the probability density function of g and is given by [15]

$$p(g) = \frac{1}{(M-1)!} g^{M-1} e^{-g} \tag{4.30}$$

with the normalization of $E\left[\left(a_{q,0}^{(k)}\right)^2\right] = 1$.

4.5.2 Analysis of Conventional PIC Receiver

For the CPIC detector, the interference cancellation is performed by subtracting the estimated signals of the interfering users from the reference signal $r_q(n)$ to form a new signal $x_q^{(1)}(n)$, which is given by

$$x_q^{(1)}(n) = r_q(n) - \sum_{k=2}^{K} s_q^{(k)}(n) \tag{4.31}$$

where $s_q^{(k)}(n)$ was defined in Eq. (4.14). The output signal after the MRC combining is given by

$$\hat{Z}^{(1)} = \Re\left[\sum_{m=1}^{M} \sum_{n=0}^{N-1} x_q^{(1)}(n) c^{(1)}(n) \left[z_{q,0}^{(1)}\right]^* \right]$$

$$= D + n_t + I'_{MAI} \tag{4.32}$$

The desired signal D and the noise term n_t are the same as the terms defined in Eq. (4.22) and Eq. (4.23), respectively. The new term I'_{MAI} is given by

$$I'_{MAI} = \sum_{m=1}^{M}\sum_{k=2}^{K}\sum_{n=0}^{N-1} c^{(k)}(n)c^{(1)}(n)\sqrt{\frac{P_k}{2M}}(d_{p,0}^{(k)} - \hat{d}_{p,0}^{(k)}) \cdot a_{q,0}^{(k)} a_{q,0}^{(1)} \cos(b_{q,0}^{(k)} - b_{q,0}^{(1)}) \quad (4.33)$$

Since [32]

$$\Pr\left[\hat{d}_{p,j}^{(k)} = d_{p,j}^{(k)} \mid d_{p,j}^{(k)}\right] = 1 - P_{ini}[e] \quad (4.34)$$

$$\Pr\left[\hat{d}_{p,j}^{(k)} = -d_{p,j}^{(k)} \mid d_{p,j}^{(k)}\right] = P_{ini}[e] \quad (4.35)$$

where $P_{ini}[e]$ is the BER of the initial stage, defined in Eq. (4.29). Thus,

$$\Pr\left[\tilde{d}_{p,j}^{(k)} = 0 \mid d_{p,j}^{(k)}\right] = 1 - P_{ini}[e] \quad (4.36)$$

$$\Pr\left[\tilde{d}_{p,j}^{(k)} = 2d_{p,j}^{(k)} \mid d_{p,j}^{(k)}\right] = P_{ini}[e] \quad (4.37)$$

Denoting $\tilde{d}_{p,j}^{(k)} = d_{p,j}^{(k)} - \hat{d}_{p,j}^{(k)}$, we have

$$E\left[\left(\tilde{d}_{p,j}^{(k)}\right)^2\right] = 4P_{ini}[e] \quad (4.38)$$

From Eq. (4.27) and Eq. (4.38), the variance of I'_{MAI} can be written as

$$Var\left[I'_{MAI}\right] = 4P_{ini}[e]Var\left[I_{MAI}^{(s)}\right] \quad (4.39)$$

The corresponding BER can then be found by using Eq. (4.28) and Eq. (4.29), with I_{MAI} replaced by I'_{MAI}.

4.5.2 Analysis of Adaptive PIC receiver

Denoting $\Delta r_q(n)$ as the difference between the reference signal $r_q(n)$ and the combined estimated signal $\sum_{k=1}^{K}\hat{v}_q^{(k)}(n)$ such that

$$r_q(n) = \sum_{k=1}^{K}\hat{v}_q^{(k)}(n) + \Delta r_q(n) \quad (4.40)$$

and using Eq. (4.9), we have

$$h_t(n) + \sum_{k=1}^{K} v_q^{(k)}(n) = \sum_{k=1}^{K} \hat{v}_q^{(k)}(n) + \Delta r_q(n)$$

$$\Delta r_q(n) = \sum_{k=1}^{K} \Delta v_q^{(k)}(n) + h_t(n) \tag{4.41}$$

where $\Delta v_q^{(k)}(n) = v_q^{(k)}(n) - \hat{v}_q^{(k)}(n)$. Hence $x_q^{(1)}(n)$ of Eq. (4.31) can be rewritten as

$$\begin{aligned} x_q^{(1)} &= r_q(n) - \sum_{k=1}^{K} \hat{v}_q^{(k)}(n) + \hat{v}_q^{(1)}(n) \\ &= \Delta r_q(n) + \hat{v}_q^{(1)}(n) \\ &= \Delta r_q(n) - \Delta v_q^{(1)}(n) + v_q^{(1)}(n) \end{aligned} \tag{4.42}$$

Thus, the soft output of the PIC-MRC stage is given by

$$\widetilde{Z}^{(1)} = \sum_{m=1}^{M} \sum_{n=0}^{N-1} v_q^{(1)}(n) c^{(1)}(n) \left[z_{q,0}^{(1)} \right]^* + \sum_{m=1}^{M} \sum_{n=0}^{N-1} \left[\Delta r_q(n) - \Delta v_q^{(1)}(n) \right] c^{(1)}(n) \left[z_{q,0}^{(1)} \right]^* \tag{4.43}$$

The first term on the RHS of Eq. (4.43) is the desired signal, identical with *D* in Eq. (4.22), while the second term is the interference, denoted as *I*, that is approximated as a zero mean Gaussian random variable. From Eq. (4.41), with the assumption that $\Delta v_q^{(k)}(n)$ is also independent and identically distributed random variable, we can have

$$E\left[\left(\Delta r_q(n) \right)^2 \right] = K \cdot E\left[\left(\Delta v_q^{(k)}(n) \right)^2 \right] + \sigma_h^2 \tag{4.44}$$

where σ_h^2 is the variance of $h_t(n)$ in Eq. (4.11). Thus,

$$E\left[\left(\Delta r_q(n) - \Delta v_q^{(1)}(n) \right)^2 \right] = (K-1) E\left[\left(\Delta v_q^{(k)}(n) \right)^2 \right] + \sigma_h^2 \tag{4.45}$$

Substituting Eq. (4.44) into Eq. (4.45) gives

$$E\left[\left(\Delta r_q(n) - \Delta v_q^{(1)}(n) \right)^2 \right] = \frac{(K-1) E\left[\left(\Delta r_q(n) \right)^2 \right] + \sigma_h^2}{K} \tag{4.46}$$

Therefore, the variance of the interference term is given by

$$Var[I] = \sum_{m=1}^{M} \left[\alpha_{q,0}^{(1)} \right]^2 \cdot \frac{(K-1) E\left[\left(\Delta r_q(n) \right)^2 \right] + \sigma_h^2}{2K} \tag{4.47}$$

where the term $E\left[\left(\Delta r_q(n)\right)^2\right]$ is the mean square error (*MSE*) of the MAI estimation and this value can be obtained from the simulation. The corresponding BER of the APIC receiver can then be found by using Eq. (4.28) and Eq. (4.29) with $Var\left[Z^{(1)}\right]$ replaced by $Var[I]$. Similarly, in the simulation we can also obtain the value of $E\left[\left(\Delta r_q(n)\right)^2\right]$ for the CPIC by setting $w_q^{(k)}(N-1)=1$ in the MAI estimation stage. Therefore, both the APIC and the CPIC receiver have the same BER expression and the only factor that causes their performance difference is $E\left[\left(\Delta r_q(n)\right)^2\right]$. The objective of adopting the adaptive algorithm in this proposed receiver is to reduce the value of $E\left[\left(\Delta r_q(n)\right)^2\right]$ in order to improve the performance.

The value of the MSE can also be obtained in theory. For simplicity, we can assume that:

$d_{p,j}^{(k)}$ are i.i.d. r.v.'s, i.e., $E\left[d_{p,j}^{(k)} d_{p,j}^{(l)}\right]=d_{k,l}$.

$d_{p,j}^{(k)}$ and $\hat{d}_{p,j}^{(k)}$ are uncorrelated, i.e., $E\left[d_{p,j}^{(k)} \hat{d}_{p,j}^{(l)}\right]=0, \quad k \neq l$.

All users have the same normalized transmission power, i.e., $P_k=1$ for all *k*'s.

The channel auto-covariance is normalized to be 1, i.e., $E\left[\left|z_{p,j}^{(k)}\right|^2\right]=1$.

The step-size is properly selected such that the misadjustment [33] of the LMS algorithm is less than 10%.

With these assumptions we can have the expression of the MSE as derived in Appendix B, which is presented by

$$MSE=\left(1+\frac{mK}{2MN}\right)\left\{\frac{K\left[1-\left(1-2P_{ini}[e]\right)^2\right]}{2MN}+s_h^2\right\} \tag{4.48}$$

where m is the step-size, *K*, *M*, *N* is the number of users in the system, the identical-bit streams and the PG, respectively. $P_{ini}[e]$ has been defined in Eq.(4.29) and $s_h^2=N_0/2$.

4.6 Numerical Results

Equation (4.48) allows the calculation of the theoretical variance of Eq. (4.47), which in turn gives an analytical upper-bound BER. The investigation reveals that this bound approaches the BER of the conventional PIC receiver. More accurate results can be achieved by using the MSE obtained from the simulation. That can be seen in Figure 4.7. A comparison of the theoretical and simulation results of the MF-MRC receiver, the CPIC receiver and the APIC receiver is shown in Figure 4.8, where the analytical result of the APIC is obtained by using the MSE derived from the simulation. Good agreement between the theoretical and simulation curves can be observed. Perfect channel estimation has been assumed and ideal power control has been applied to simplify the calculation of the theoretical results.

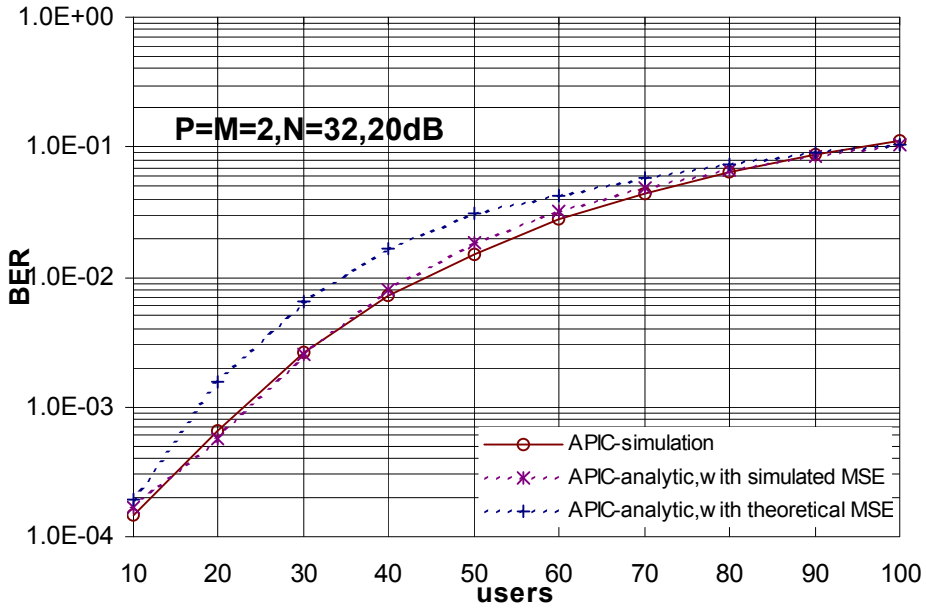

Figure 4.7 Theoretical and simulation results of the APIC receiver for synchronous MC-DS-CDMA

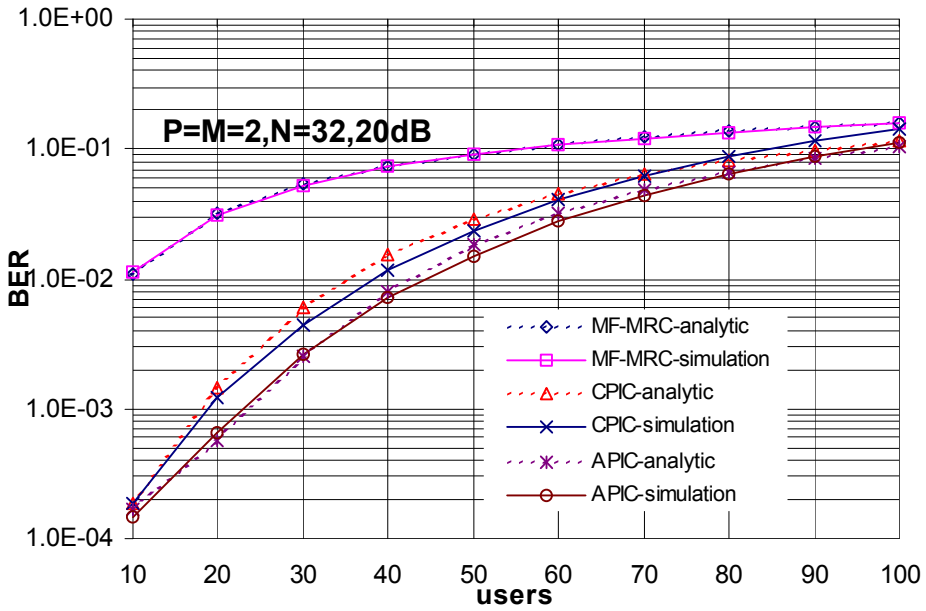

Figure 4.8 Comparison of the analytic and simulation results of the MF-MRC, CPIC and APIC receivers for synchronous MC-DS-CDMA

Chapter 5

Simulation Results and Discussions for Synchronous MC-DS-CDMA System

5.1 Simulation Environment (Method and Model)

For evaluating the theoretical results and to investigate the performance of the system under various circumstances, simulation work has been carried out. A method called "Monte Carlo simulations" is performed using the C compiler. Monte Carlo simulation is simply a sequence of Bernoulli trials where one performs multiple independent experiments and computes an ensemble average by counting the number of successes (or errors) and dividing by the number of trials [34]. It is desirable for analyzing complex systems such as those employing multiuser detection because they allow the underlying system architecture to be closely modeled. A distinctive feature of these types of simulations is the large amount of computer time required to generate accurate bit error estimates. In this study, we typically run simulations such that approximately 50-100 errors are observed, before the BER is quantified.

Matlab functions are utilized to verify some functions generated in C programs. For example, to verify the Rayleigh fading generation function in C program, we can get the probability density function (pdf) of the random variables generated by C and plot out its pdf curve; if this figure can match the pdf curve generated from the

function of *raylpdf( )* in Matlab, we can assert that the Rayleigh fading generation function in C program is correct. Other software such as *Mathematica* is also adopted to calculate the complex mathematical expressions such as Eq. (4.47). In this thesis, each simulation result on the BER of different receivers has its theoretical counterpart, thus ensuring the effectiveness of the simulations.

The numerical examples of this thesis depend on the use of random codes. The transmitting data of all users randomly take on the binary value of 0 and 1, with equal probability. BPSK modulation is adopted in all the simulation programs, thus mapping the 0 and 1 to –1 and +1, respectively. These data are spread by the signature sequence. Although the chip sequence is usually deterministic and periodic (although the sequence appears random within a period), analysis is sometimes simplified by assuming that the signature sequence is completely random; that is, the pulses are generated from a random process producing outcomes uniform on the set $\{-1, +1\}$. During the demodulation process at the receiver, the composite signal is multiplied by a synchronous replica of the original signature sequence. The two sequences are thus cancelled, and the desired data resulting at the integrator are the output [37]. It is shown in [38] that in the frequency selective fading channel, the random codes provide a performance between the best and the worst choice of codes. The long codes used in the simulations are the scrambling codes with a period of $2^{25}-1=33554431$ according to the IMT2000 standard. The generation of two certain long scrambling codes is shown in Appendix C. Altogether there are 2^{24} long codes according to this method, with 2^{24} different initial conditions for x sequence as shown in Appendix C.

Since only an uncoded system is studied, the data are directly transmitted after spreading. These signals are subjected to distortions due to fading and shadowing

characterizing the mobile environment. Hence, an appropriate channel model constitutes a crucial component for the performance simulations.

The mobile radio channel is usually evaluated using statistical propagation models where the channel parameters are modeled as stochastic variables [15]. A common approach in describing the channel is to assume that the transmitted radio waves, causing the interference pattern, act as plane wave fronts from different directions, due to the multipath propagation. A statistical description of such mobile radio channels has been developed by Clarke [39] and Jakes [40]. The property of the channel is deduced from a scattering propagation model which assumes that the field incident to the receiver antenna is composed of an infinite number of randomly phased azimuthal plane waves of arbitrary azimuthal angles. The Jakes model and its relationship with the Rayleigh density formula are presented in Appendix D.

In the simulations, the channel is assumed to be fading slowly. This means very small Doppler shift is observed such that it can be assumed that the fading gain over one symbol is constant. To simplify the case, perfect channel estimation is assumed in this thesis. Power control is also applied such that the received power is equal for all users. As mentioned before, the principle motivation for MC systems is to allow a frequency selective fading channel to appear as flat fading on each subcarrier. It is assumed that the fading gain is uncorrelated and identically distributed for different user and subcarrier. This is a slight simplification over a real channel which would be correlated in frequency, but typically the difference in performance for correlated modeling is small. Investigation in [27] has shown that only large subcarrier correlation coefficients result in an obvious worsening of the performance. It is also shown in [41-42] that nonindependent fading is also very effective. Therefore, in order

to simplify the case, the fading gain on each subcarrier is independent and identically distributed for all the simulations of this thesis.

5.2 Results and Discussion

Simulation Results were obtained based on the models and assumptions mentioned above. The advantage of MC-DS-CDMA over SC-DS-CDMA is shown in Figure 5.1. In this case, for the SC-DS-CDMA system, the channel is frequency selective Rayleigh fading with the number of multipath $L' = 3$, and a uniform power profile is considered. A RAKE receiver, which is assumed to be able to capture all the three paths, is utilized to recover all the energy. For the MC-DS-CDMA system, according to Eq. (4.5), if the parameters of the transmitter are chosen to be $P = M = 2$, thus $L = 1$, i.e., each subcarrier undergoes a frequency non-selective fading. The PG of the SC-DS-CDMA system for Figure 5.1 is 64. From Eq. (4.4), the PG of the MC-DS-CDMA system should be approximately 52 in order to keep the bandwidth constant.

The BER plotted against the user capacity for the RAKE receiver of the SC-DS-CDMA and the MF-MRC receiver of the MC-DS-CDMA system is shown in Figure 5.1. From the figure we can see that the performance of the MC-DS-CDMA system with matched filter is better than that of the SC-DS-CDMA system with RAKE receiver. At a BER of 10^{-2}, the MC-DS-CDMA system with matched filter can support nearly 10% more users than the SC-DS-CDMA system with RAKE receiver. This benefit is the result of the overlapping spectrum of the MC-DS-CDMA system. Theoretically, a single carrier CDMA system in an L' multipath channel with an ideal RAKE receiver is equivalent to a MC system with L' carriers having nonoverlapping frequency spectrums. In both cases, L' replicas with approximately independent fading envelopes are available at the output of the channel [6]. While in the MC system here,

more narrowband signals can be added since their spectra overlap with the originally nonoverlapping signals. Hence higher spectrum efficiency can be achieved regardless the correlation between the nonindependent faded envelopes.

When the MAI cancellation techniques are adopted in the MC-DS-CDMA system, further performance improvement can be achieved. Figure 5.1 also gives the performance of the one- and two-stage CPIC and APIC receivers. At an SNR of 20 dB, it is shown that for the one-stage CPIC receiver in the MC-DS-CDMA system, the capacity is increased to 4.3 times as compared to that of the MF-MRC receiver at the BER of 10^{-2}. At the same BER, from the figure, one-stage APIC is able to accommodate about 15% more users than the one-stage CPIC receiver. The two-stage APIC receiver can contain about 17% more users than the two-stage CPIC. Note that the step-size m for one-stage APIC receiver is 0.1. For the two-stage APIC receiver, the first stage uses the step-size of 0.1 and the second stage 0.05. The initial weights are all set to be 1.

In addition, Figure 5.1 also shows the advantage of frequency diversity in the MC-DS-CDMA system, (i.e., $M > 1$). The performance of the CPIC and the APIC receiver in the MC-DS-CDMA without diversity ($M = 1$) is plotted in dash-line curves. P is chosen to be *4* and the PG is *104* so that the number of carriers and the bandwidth are the same as the system with $P = M = 2$ and $N = 52$. We can see that the performance of the MC-DS-CDMA system improves when diversity is introduced.

Figure 5.2 shows the performance comparison of one-stage APIC with one-stage CPIC. BER versus SNR curves are plotted with a PG of 32. The three groups of curves represent the performance of APIC and CPIC with 10 users, 40 users, and 70 users respectively. It is shown in the figure that for the system with 10 users, the APIC is only able to outperform the CPIC when the SNR is larger than 20dB. This means that

the APIC has an advantage over the CPIC only when the SNR is high, under the condition that there is only a small number of users in the system. This can be explained in a straightforward manner if we recognized that the difference between the APIC and the CPIC receivers is the MAI estimation stage. It is by estimating the interference more precisely that the APIC receiver can subtract more MAI and hence achieve better performance. If the system is noise dominant, the MAI estimation stage shifts to an insignificant role.

There are other factors that are affecting the performance of the APIC receiver, such as the value of step-size m and the initial weights. The effect of selecting the value of the initial weights and the step-size on the performance of the APIC is shown in Figure 5.3.

Figure 5.3 shows the BER performance of the one-stage APIC receiver with 30 users at SNR of 20dB, and the PG is 32. At a certain initial weight, for example, $w = 1$, when the step-size sweeps from nearly 0 to 1.5, there is a minimum point for the performance curve at $m = 0.3$. For different initial weights, the minimum points are different. We can see from the figure that the minimum point is the lowest when the initial weight is 1. Note that if the initial weight is 1 and the step-size is 0, this APIC receiver becomes the CPIC receiver.

In Figure 5.4, the BER performance of the one- and two-stage of the APIC receiver versus the step-size m is presented. The initial weight has been fixed at 1 and the SNR is 20dB. The PG equals to 32. When the number of users is 30, the one-stage APIC receiver achieves its best performance at $m = 0.3$. However, for the two-stage APIC receiver (with the step-size of the first stage, $m_1 = 0.3$), the best performance is at the point where $m = 0$ (the APIC becomes the CPIC) for the second stage. This means the CPIC is more effective than the APIC for the second stage in this case. When the

number of users *K* is increased to 100 and $m_1 = 0.3$, one can observe that the best BER performance is at the point $m = 0.3$ for the second stage of the two-stage APIC. The results show that the advantage of using the APIC beyond the first stage of the multi-stage interference cancellation structure is only apparent when the level of MAI is high.

The influence of the initial weight and the PG used on the performance of the adaptive algorithm in the APIC will be discussed below. Figure 5.5 shows the convergence comparison for different initial weights for the one-stage APIC receiver with 30 users at an SNR of 20dB, PG 32, and the step-size is fixed at 0.3. From Figure 5.5, when the initial weight is 0, the adaptive algorithm does not converge to its minimum point at the end of one bit period (note that in this APIC scheme, the number of iterations is equal to the PG). But when the initial weight is 1, the MSE floor is the lowest.

However, when the PG is increased to 256 (consequently, the number of iterations is 256) with other parameters unchanged, in Figure 5.6, the MSE for different initial weights converge to almost the same error floor. These results show that it is critical to choose the appropriate initial weights when the PG is low in order to ensure the effectiveness of this APIC scheme.

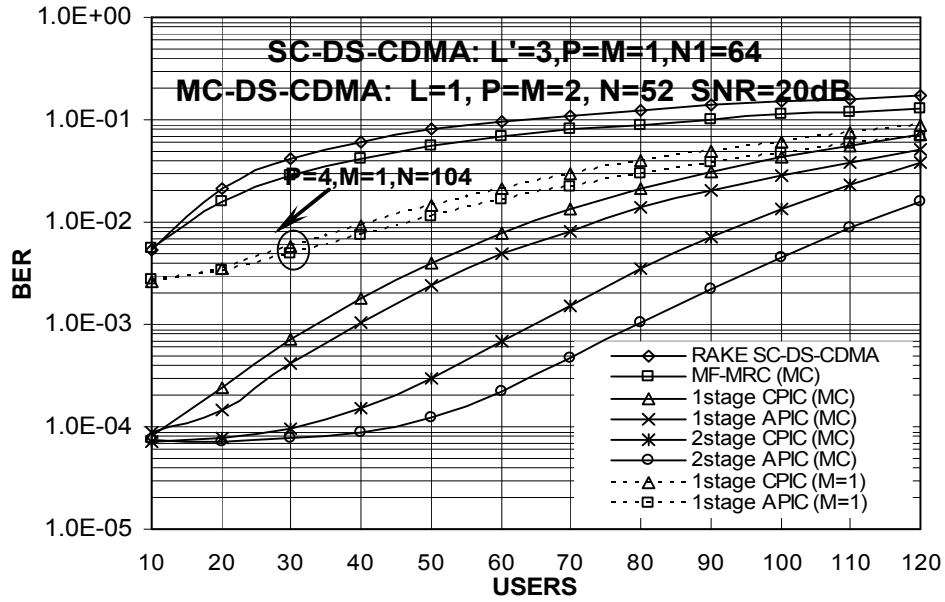

Figure 5.1 BER Performance of various receivers in Rayleigh fading channel at SNR of 20dB for synchronous MC-DS-CDMA.

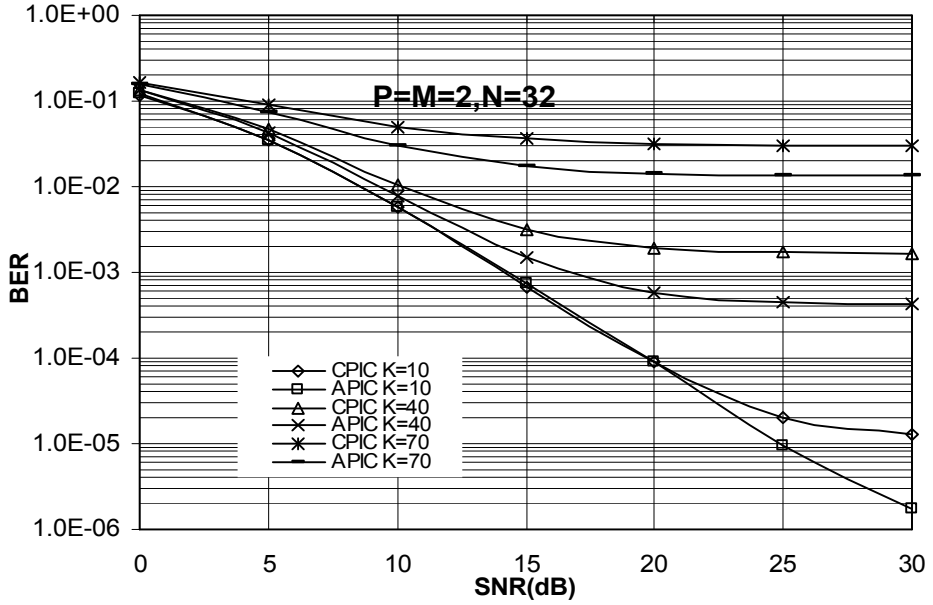

Figure 5.2 BER performance of one-stage PIC receivers as a function of SNR for synchronous MC-DS-CDMA system

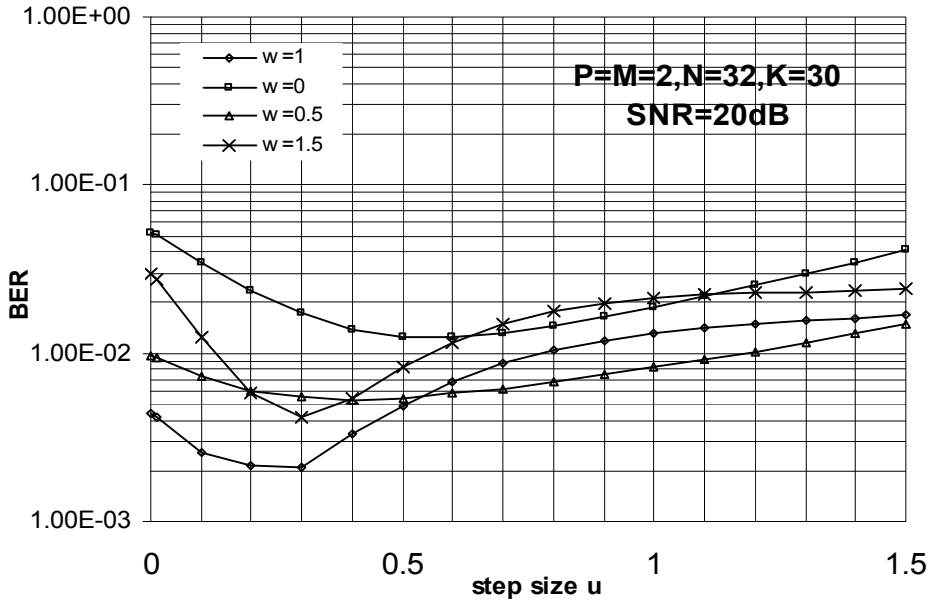

Figure 5.3 BER performance of one-stage APIC receiver with different initial weights as a function of step-size for MC-DS-CDMA system.

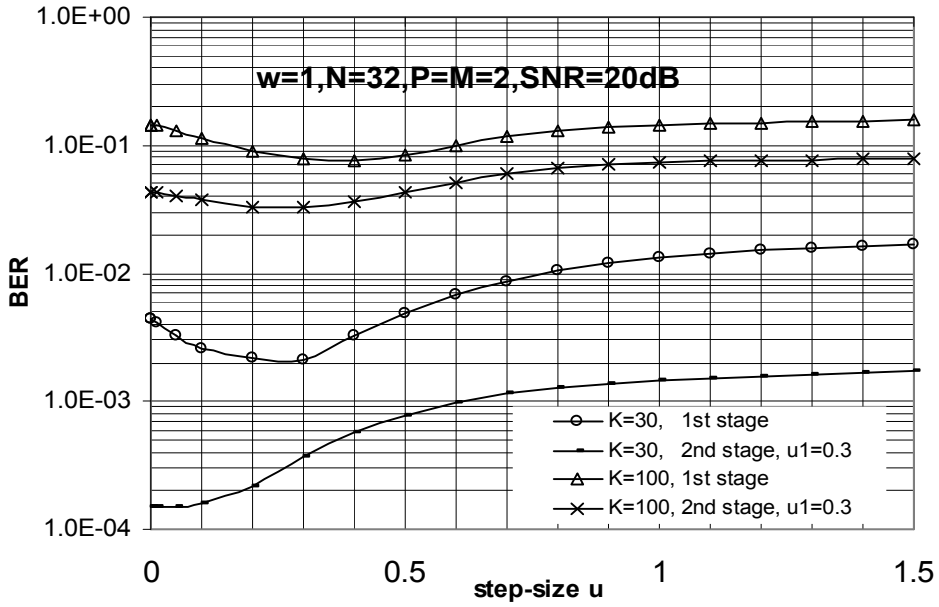

Figure 5.4 BER performance of the first and second stage of the APIC Vs. step-size

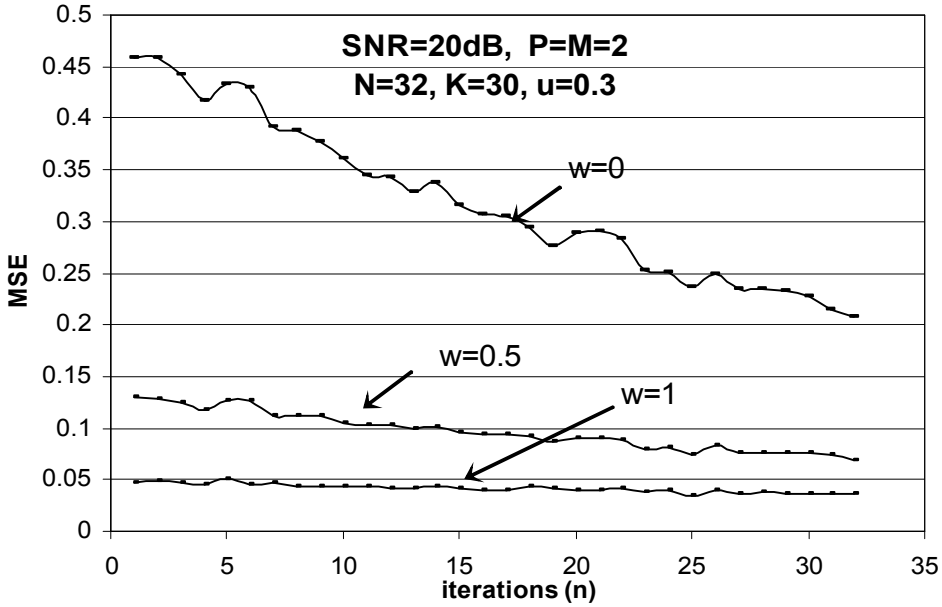

Figure 5.5 Convergence comparison for different initial weights for the one-stage APIC receiver with 30 users at SNR of 20dB, PG 32, step-size 0.3.

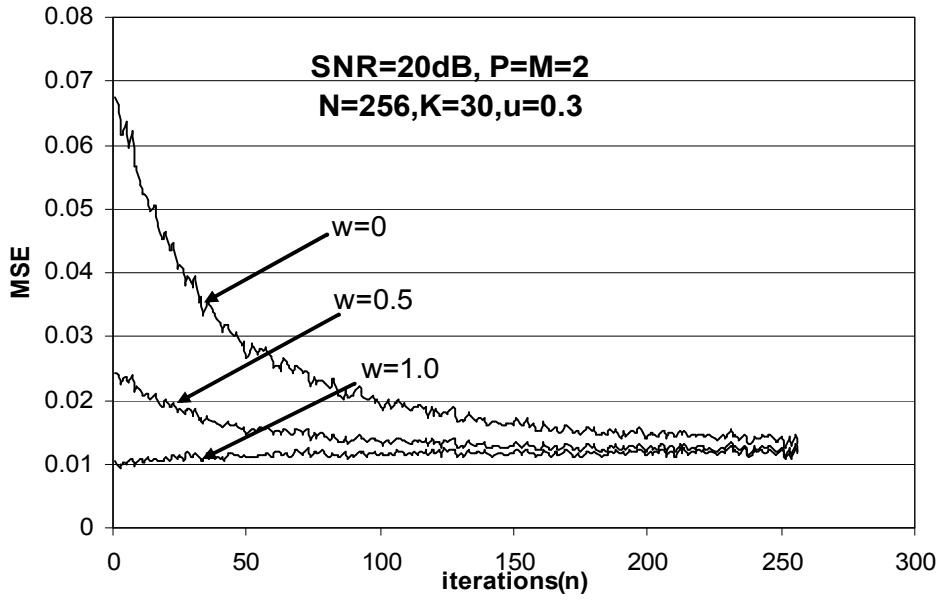

Figure 5.6 Convergence comparison for different initial weights for the one-stage APIC receiver with 30 users at SNR of 20dB, PG 256, step-size 0.3.

Chapter 6

APIC Receiver for Asynchronous MC-DS-CDMA System

In the previous two chapters, only the synchronous case was studied. Actually there are two methods to build the structure of the synchronous APIC receiver, depending on the choice of the reference signal of the adaptive algorithm. One method is what we have adopted in Chapter 4 and Chapter 5. That scheme is a subcarrier-based program, which uses the demodulated signal on each subcarrier as the reference and subsequently processes the signals with MRC combining. It simplifies the structure of the receiver by taking advantage of the synchronization of all users. All users' data arrive at the receiver without any time offset between each other, thus the signal can be coherently demodulated with only one FFT block. By using the demodulated signal as the reference for the adaptive algorithm, the demand on the subcarriers' reconstruction is avoided. Therefore the cost of building a receiver has significantly been reduced by minimizing the number of IFFT and FFT blocks.

The other scheme is to use the composite received signal as the reference of the adaptive algorithm and reconstruct the signals by using K IFFT blocks before the MAI estimation stage. The same number of FFT blocks is needed to re-modulate the signals in the PIC stage. This scheme is not so economical although its performance is fairly good.

However, for the asynchronous channel, only the second scheme can be adopted due to the time mis-alignment between users. The system model and the performance will be presented below.

6.1 System Model

Similar to the transmitter structure in Chapter 4, the transmitting bit stream is converted into *P parallel-bit* branches. Each parallel branch data is copied into *M* identical-bit streams. These streams are all spread by the same pseudo random spreading sequences that uniquely identify each user in the system. Each stream is then assigned a carrier that is orthogonal to each other.

Invoking power control among the users, the channel is assumed to be statistically identical for all users. For simplicity, as described in the synchronous case, we choose the bandwidth of each subcarrier in the multicarrier system to be less than the coherence bandwidth of the channel and assume that the various subcarriers transmitted by a given user are subject to uncorrelated fading. The complex channel gain for the qth carrier of user k is denoted as $z_q^{(k)}(t) = a_q^{(k)}(t)\exp\left[b_q^{(k)}(t)\right]$, where $\left\{a_q^{(k)}(t)\right\}$ is a Rayleigh-distributed stochastic process with unit second moment while $\left\{b_q^{(k)}(t)\right\}$ is uniformly distributed over 0 and $2p$.

In this chapter, an asynchronous MC-DS-CDMA system of K users with BPSK modulation on each carrier is considered. The received signal $r(t)$ is given by

$$r(t) = \sum_{k=1}^{K}\sum_{j=-\infty}^{\infty}\sum_{p=1}^{P}\sum_{m=1}^{M}\sqrt{\frac{2P_k}{M}}d_{p,j}^{(k)}p_{T_b}(t - jT_b - \tau_k)c^{(k)}(t-\tau_k)$$

$$\cdot a_{q,j}^{(k)}\cos(\omega_q t + \theta_{q,j}^{(k)}) + n(t), \qquad (6.1)$$

where P_k is the power of the kth user, $d_{p,j}^{(k)}$ is the jth bit of the kth user's pth parallel-

bit branch, $p_l(t)$ is a rectangular pulse waveform with unit amplitude and duration l, w_q is the qth carrier frequency, and $c^{(k)}(t)$ is the spreading sequence of user k, which is given by

$$c^{(k)}(t) = \sum_{n=-\infty}^{\infty} c^{(k)}(n) p_{T_c}(t - nT_c) \tag{6.2}$$

where $c^{(k)}(n)$ being the n^{th} chip of the spreading sequence of the user k and T_c is the chip duration. The spreading sequence is normalized such that $\int_0^{T_b} \left[c^{(k)}(t)\right]^2 dt = 1$. Note that we have assumed that the channel is fading slowly such that the channel gain $z_q^{(k)}(t)$ remains constant for a bit duration. Hence instead of denoting it as function of time, a subscript j is introduced so that now $z_{q,j}^{(k)} = a_{q,j}^{(k)} \exp\left[b_{q,j}^{(k)}\right]$ represents the channel gain at the jth symbol. The delay t_k due to asynchronous transmission is uniformly distributed in $[0, T_b)$ so that the maximum delay between any two users is less than a bit duration. The term $q_{q,j}^{(k)} = b_{q,j}^{(k)} - w_q t_k$ is uniformly distributed between 0 and $2p$, which consists of both the phase of the channel gain and the phase caused by the propagation delay. The parameter $q = p + (m-1)P$ is the carrier number index corresponding to the pth parallel-bit branch and mth identical-bit stream. Lastly $n(t)$ is the additive white Gaussian noise (AWGN) with zero mean and double-sided power spectral density of $N_0/2$.

6.2 Receiver Structure

Referring to Figure 6.1, the structure of the proposed receiver can be depicted in four steps.

Firstly, after the received signal is down converted to its equivalent baseband signal, it is passed through each user's subcarrier demodulator, i.e., the FFT block in the front end of the receiver. The output signals of the corresponding user's FFT block can be grouped into P sets, each comprising of the M identical-bit streams. These signals are passed into the corresponding MF and then the diversity streams are combined together by MRC to produce the tentative decisions.

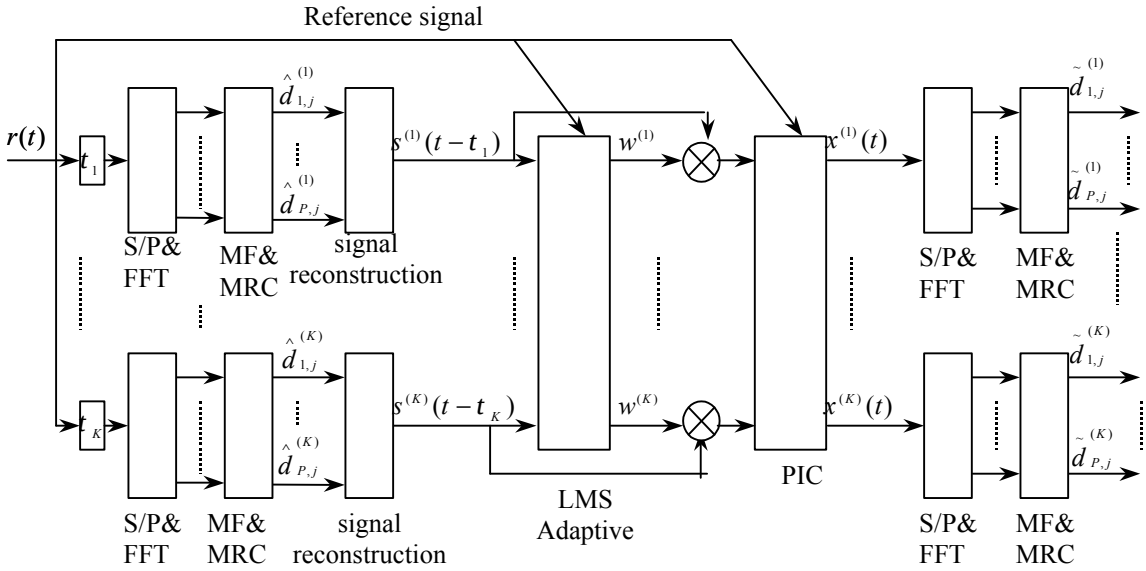

Figure 6.1 Receiver structure for the asynchronous MC-DS-CDMA system

Without loss of generality, we can assume user 1 is the intended user and thus let $t_1 = 0$. Hence the tentative decision of the 0^{th} bit of the hth parallel branch for user 1 is given by

$$\hat{d}_{h,0}^{(1)} = sign\{Z_{h.0}^{(1)}\}, \tag{6.3}$$

where

$$Z_{h,0}^{(1)} = \sum_{l=1}^{M} \int_0^{T_b} r(t)\cos(w_i t + q_{i,0}^{(1)})c^{(1)}(t)a_{i,0}^{(1)}dt \tag{6.4}$$

and $i = h + (l-1)P$ is the carrier number index corresponding to the hth parallel-bit

branch and the *l*th identical-bit stream.

Secondly, based on the tentative decision, M copies of $\hat{d}_{h,j}^{(k)}$, which constitute the identical-bit streams are reconstructed. Each of these M copies are spread with the corresponding user's spreading code $c^{(k)}(t)$ and multiplied with the corresponding channel gain. These reconstructed signals are then passed through the IFFT circuit. If perfect channel and timing estimation and ideal power control are assumed, the output signal of the *k*th user after the reconstruction phase can be written as

$$s^{(k)}(t-\tau_k) = \sum_{j=-\infty}^{\infty} \sum_{i=1}^{PM} \sqrt{\frac{2P_k}{M}} \hat{d}_{h,j}^{(k)} p_{T_b}(t - jT_b - \tau_k) c^{(k)}(t-\tau_k)$$

$$\cdot a_{i,j}^{(k)} \cos(\omega_i t + \theta_{i,j}^{(k)}) \qquad (6.5)$$

The regenerated signals of all the users are multiplied by the adaptive weights $w^{(k)}(t)$ and then summed together to produce an estimation of the received signal $r(t)$. These weights are adjusted based on the normalized LMS algorithm [31] that operates over a two-bit interval. The reason for taking a two-bit window is because we have assumed the maximum delay between two users is less than one bit, as mentioned previously. The number of iterations depends on the sampling rate and the window duration. At the end of the iterations, the final weights w_k are obtained, which will be used by the next stage of the receiver, as described below. Note that for the CPIC receiver, there is no adaptive process involved. Hence this is equivalent to setting $w_k = 1$ for all users.

Thirdly, at the interference cancellation step, the final weights w_k will be used to multiply the input signals $s^{(k)}(t-\tau_k)$ over the entire two-bit interval. Hence the interference cancellation for user one is performed as

$$x^{(1)}(t) = r(t) - \sum_{k=2}^{K} \hat{v}^{(k)}(t), \qquad (6.6)$$

where

$$\hat{v}^{(k)}(t) = s^{(k)}(t - \tau_k) w_k . \tag{6.7}$$

Lastly, the same operations as in the first step are performed in this final step, with the input signal being $x^{(1)}(t)$ instead of $r(t)$. Hence the final decision for user one is then given by

$$\tilde{d}_{h,0}^{(1)} = sign\left\{\tilde{Z}_{h,0}^{(1)}\right\}. \tag{6.8}$$

where the expression of $\tilde{Z}_{h,0}^{(1)}$ can be found by replacing $r(t)$ with $x^{(1)}(t)$ in Eq. (6.4).

In Figure 6.1, if the final decisions are taken after the first stage, then the structure becomes the MF receiver. However if we consider the entire receiver structure but set the weight $w_k = 1$ in the interference cancellation step, then the receiver becomes the CPIC receiver. For comparison purpose, the performance analysis of the MF receiver, the CPIC receiver and the APIC receiver will be presented in the next section.

6.3 Performance Analysis

6.3.1 Performance of the matched filter (MF) receiver

The analysis of the performance of the MF receiver is similar to [6]. As mentioned above, the soft output of the matched filter for user one is given in Eq. (6.4) and it can be further expressed by

$$Z_{h,0}^{(1)} = D + h + I_{MAI} \tag{6.9}$$

where

$$D = \sqrt{\frac{P_1}{2M}} d_{h,0}^{(1)} \sum_{l=1}^{M} \left[a_{i,0}^{(1)}\right]^2 \tag{6.10}$$

and

$$h = \sum_{l=1}^{M} \int_0^{T_b} n(t)c^1(t)\cos(w_i t + q_{i,0}^{(1)})a_{i,0}^{(1)} dt \tag{6.11}$$

is a Gaussian random variable with zero mean and variance given by

$$s_h^2 = \frac{N_0}{4} \sum_{l=1}^{M} \left[a_{i,0}^{(1)}\right]^2 . \tag{6.12}$$

The term I_{MAI} in Eq. (6.9) is the MAI, which can be expressed as a combination of two components, denoted as $I_{MAI}^{(s)}$ and $I_{MAI}^{(d)}$. $I_{MAI}^{(s)}$ refers to the interference from the other users on the same carrier, which is given by

$$\begin{aligned} I_{MAI}^{(s)} &= \sum_{l=1}^{M} \int_0^{T_b} \sum_{k=2}^{K} \sum_{j=-\infty}^{\infty} \sqrt{\frac{2P_k}{M}} d_{h,j}^{(k)} p_{T_b}(t - jT_b - t_k) a_{i,j}^{(k)} c^{(k)}(t - t_k) \\ &\quad \cos(w_i t + q_{i,j}^{(k)}) \cdot \cos(w_i t + q_{i,0}^{(1)}) c^{(1)}(t) a_{i,0}^{(1)} dt \\ &= \sum_{l=1}^{M} \sum_{k=2}^{K} \sqrt{\frac{P_k}{2M}} a_{i,0}^{(1)} \\ &\cdot \left[d_{h,-1}^{(k)} a_{h,-1}^{(k)} R_{k,1}(t_k) \cos(q_{i,-1}^{(k)} - q_{i,0}^{(1)}) + d_{h,0}^{(k)} a_{h,0}^{(k)} \hat{R}_{k,1}(t_k) \cos(q_{i,0}^{(k)} - q_{i,0}^{(1)}) \right] \end{aligned} \tag{6.13}$$

where $R_{k,1}(t_k)$ and $\hat{R}_{k,1}(t_k)$ are the continuous time partial cross-correlation defined in [43]. $I_{MAI}^{(s)}$ can be approximated as a Gaussian random variable with zero mean having a variance given by

$$Var\left[I_{MAI}^{(s)}\right] = \frac{1}{6MN^3} \sum_{k=2}^{K} P_k r_{k,1} \sum_{l=1}^{M} \left[a_{i,0}^{(1)}\right]^2 , \tag{6.14}$$

where $r_{k,1}$ is defined in [43]. $I_{MAI}^{(d)}$ is the interference from the other users on different carriers, which is given by

$$\begin{aligned} I_{MAI}^{(d)} &= \sum_{l=1}^{M} \int_0^{T_b} \sum_{k=2}^{K} \sum_{j=-\infty}^{\infty} \sum_{\substack{q=1 \\ q \neq i}}^{PM} \sqrt{\frac{2P_k}{M}} d_{h,j}^{(k)} p_{T_b}(t - jT_b - t_k) c^{(k)}(t - t_k) \\ &\quad a_{q,j}^{(k)} \cos(w_q t + q_{q,j}^{(k)}) \cdot \cos(w_i t + q_{i,0}^{(1)}) c^{(1)}(t) a_{i,0}^{(1)} dt . \end{aligned} \tag{6.15}$$

Similar to [6], $I_{MAI}^{(d)}$ is assumed to be a Gaussian random variable with zero mean

having a variance

$$Var\left[I_{MAI}^{(d)}\right]=\sum_{k=2}^{K}\frac{P_k\left(m_{k,1}(0)-m_{k,1}(1)\right)}{2p^{2}MN^{3}}\sum_{l=1}^{M}\left[a_{i,0}^{(1)}\right]^{2}\sum_{\substack{q=1\\q\neq i}}^{PM}\frac{1}{(q-i)^{2}} \tag{6.16}$$

where $m_{k,1}(0)$ and $m_{k,1}(1)$ are defined in [43]. From Eq. (6.9-6.15), assuming that a bit '1' is transmitted, the mean and variance of $Z_{h,0}^{(1)}$ conditioned on a set of M Rayleigh random variables, denoted here as $\left\{a_{i,0}^{(1)}\right\}$, where $i=h+(l-1)P, l=1,\cdots,M$ are given by

$$E\left[Z_{h,0}^{(1)}\middle|\left\{a_{i,0}^{(1)}\right\}\right]=\sqrt{\frac{P_1}{2M}}\sum_{l=1}^{M}\left[a_{i,0}^{(1)}\right]^{2} \tag{6.17}$$

and

$$Var\left[Z_{h,0}^{(1)}\middle|\left\{a_{i,0}^{(1)}\right\}\right]=s_h^{2}+Var\left[I_{MAI}^{(s)}\right]+Var\left[I_{MAI}^{(d)}\right], \tag{6.18}$$

respectively. Hence the probability of error associated with the hth parallel-bit branch conditioned on $\left\{a_{i,0}^{(1)}\right\}$ is given by

$$P_h\left[e\middle|\left\{a_{i,0}^{(1)}\right\}\right]=\frac{1}{2}erfc\left(\frac{E\left[Z_{h,0}^{(1)}\middle|\left\{a_{i,0}^{(1)}\right\}\right]}{\sqrt{2Var\left[Z_{h,0}^{(1)}\middle|\left\{a_{i,0}^{(1)}\right\}\right]}}\right) \tag{6.19}$$

The BER for the hth parallel-bit branch is then obtained by averaging $P_h\left[e\middle|\left\{a_{i,0}^{(1)}\right\}\right]$ over $\left\{a_{i,0}^{(1)}\right\}$ according to

$$P_h[e]=\int_0^{\infty}P_h\left[e\middle|\left\{a_{i,0}^{(1)}\right\}\right]p(a_{h,0}^{(1)},\cdots,a_{h+(M-1)P,0}^{(1)})da_{h,0}^{(1)}\cdots da_{h+(M-1)P,0}^{(1)}, \tag{6.20}$$

where $p(a_{h,0}^{(1)},\cdots a_{h+(M-1)P,0}^{(1)})$ is the joint probability density function of $\left\{a_{i,0}^{(1)}\right\}$. Assuming that any bit can be sent via any of the P parallel branches with equal probability, then the final BER can be written as

$$P_{MF}[e]=\frac{1}{P}\sum_{h=1}^{P}P_h[e] \tag{6.21}$$

6.3.2 Performance of the Conventional PIC (CPIC) Receiver

If we set the value of $w_k = 1$ in Eq. (6.7), then the receiver becomes a CPIC. In this case, the final decision associated with the *h*th parallel-bit branch of user one is based on the soft output signal $\widetilde{Z}_{h,0}^{(1)}$, which is

$$\widetilde{Z}_{h,0}^{(1)} = D + \boldsymbol{h} + I_{MAI}^{'} \tag{6.22}$$

where D and $\boldsymbol{h}$ are the same as that defined in Eq. (6.9). The term $I_{MAI}^{'}$ is similar to I_{MAI} given in Eq. (6.9), with the exception that now $d_{h,j}^{(k)}$ in Eq.(6.13-6.15) is replaced by $d_{h,j}^{(k)} - \hat{d}_{h,j}^{(k)}$.

From [32] we have the relationship of

$$\Pr\left[\hat{d}_{h,j}^{(k)} = d_{h,j}^{(k)} \mid d_{h,j}^{(k)}\right] = 1 - P_{MF}[e] \tag{6.23}$$

$$\Pr\left[\hat{d}_{h,j}^{(k)} = -d_{h,j}^{(k)} \mid d_{h,j}^{(k)}\right] = P_{MF}[e] \tag{6.24}$$

where $P_{MF}[e]$ has been defined in Eq. (6.21). Based on the above two equations, we can get

$$E\left[\left(d_{h,j}^{(k)} - \hat{d}_{h,j}^{(k)}\right)^2\right] = 4P_{MF}[e] \tag{6.25}$$

Then the variance of $I_{MAI}^{'}$ can be written as

$$Var\left[I_{MAI}^{'}\right] = 4P_{MF}[e]Var\left[I_{MAI}\right] \tag{6.26}$$

The corresponding BER can then be found by using Eq. (6.19) and Eq. (6.20), with $Var\left[Z_{h,0}^{(1)} \middle| \{\boldsymbol{a}_{i,0}^{(1)}\}\right]$ replaced with $Var\left[\widetilde{Z}_{h,0}^{(1)} \middle| \{\boldsymbol{a}_{i,0}^{(1)}\}\right]$. The BER derivation of the APIC receiver will be presented in the next section, which can also be considered as an alternative method to analyze the BER of the CPIC receiver when we set $w_k = 1$ in the APIC receiver structure.

6.3.3 Performance of the Adaptive PIC (APIC) Receiver

The analysis of the APIC receiver for asynchronous channel is quite similar to the synchronous case. Denoting $\Delta r(t)$ as the difference between the reference signal $r(t)$ and the combined estimated signal $\sum_{k=1}^{K}\hat{v}^{(k)}(t)$ such that

$$r(t)=\sum_{k=1}^{K}\hat{v}^{(k)}(t)+\Delta r(t) \tag{6.27}$$

If we let

$$v^{(k)}(t)=\sum_{j=-\infty}^{\infty}\sum_{p=1}^{P}\sum_{m=1}^{M}\sqrt{\frac{2P_k}{M}}d_{p,j}^{(k)}p_{T_b}(t-jT_b-t_k)c^{(k)}(t-t_k)$$

$$\cdot a_{q,j}^{(k)}\cos(w_q t+q_{q,j}^{(k)}), \tag{6.28}$$

where $q=p+(m-1)P$, then by using the expression in Eq. (6.27), Eq. (6.1) can be rewritten as

$$r(t)=\sum_{k=1}^{K}v^{(k)}(t)+n(t)$$

$$\sum_{k=1}^{K}\hat{v}^{(k)}(t)+\Delta r(t)=\sum_{k=1}^{K}v^{(k)}(t)+n(t)$$

$$\Delta r(t)=\sum_{k=1}^{K}\Delta v^{(k)}(t)+n(t), \tag{6.29}$$

where $\Delta v^{(k)}(t)=v^{(k)}(t)-\hat{v}^{(k)}(t)$. Hence $x^{(1)}(t)$ of Eq. (6.6) can be rewritten as

$$x^{(1)}(t)=r(t)-\sum_{k=1}^{K}\hat{v}^{(k)}(t)+\hat{v}^{(1)}(t)$$

$$=\Delta r(t)+\hat{v}^{(1)}(t)$$

$$=\Delta r(t)-\Delta v^{(1)}(t)+v^{(1)}(t) \tag{6.30}$$

At the final step, the M matched filter outputs corresponding to the hth parallel-bit branch are combined by MRC. Assuming perfect channel estimation, the soft decision statistic is then given by

$$\widetilde{Z}_{h,0}^{(1)} = \sum_{l=1}^{M} \int_0^{T_b} x^{(1)}(t)\cos(\omega_i t + \theta_{i,0}^{(1)})c^{(1)}(t)a_{i,0}^{(1)}dt$$

$$= \sum_{l=1}^{M} \int_0^{T_b} v^{(1)}(t)\cos(\omega_i t + \theta_{i,0}^{(1)})c^{(1)}(t)a_{i,0}^{(1)}dt +$$

$$\sum_{l=1}^{M} \int_0^{T_b} \left[\Delta r(t) - \Delta v^{(1)}(t)\right]\cos(\omega_i t + \theta_{i,0}^{(1)})c^{(1)}(t)a_{i,0}^{(1)}dt \qquad (6.31)$$

The first term on the RHS of Eq. (6.31) is the desired signal, which is identical to D in Eq. (6.9), while the second term is the interference, denoted as *I*, that is approximated as a zero mean Gaussian random variable. To determine the variance of *I*, we can assume that the statistics of $\Delta v^{(k)}(t)$ are independent and identically distributed for all the users. Hence,

$$E\left[\left(\Delta r(t)\right)^2\right] = K \cdot E\left[\left(\Delta v^{(k)}(t)\right)^2\right] + \sigma_n^2, \qquad (6.32)$$

where $\sigma_n^2 = N_0/2$ is the variance of $n(t)$ in Eq. (6.1). Thus,

$$E\left[\left(\Delta r(t) - \Delta v^{(1)}(t)\right)^2\right] = (K-1)E\left[\left(\Delta v^{(k)}(t)\right)^2\right] + \sigma_n^2. \qquad (6.33)$$

Substituting Eq. (6.32) into Eq. (6.33) gives

$$E\left[\left(\Delta r(t) - \Delta v^{(1)}(t)\right)^2\right] = \frac{(K-1)E\left[\left(\Delta r(t)\right)^2\right] + \sigma_n^2}{K}. \qquad (6.34)$$

Therefore the variance of the interference term is given by

$$Var[I] = \sum_{l=1}^{M}\left[a_{i,0}^{(1)}\right]^2 \cdot \frac{(K-1)E\left[\left(\Delta r(t)\right)^2\right] + \sigma_n^2}{2K} \qquad (6.35)$$

This expression is the same with Eq. (4.47); the term $E\left[\left(\Delta r(t)\right)^2\right]$ is the mean square error (MSE) of the MAI estimation. By obtaining the MSE value using simulations, the variance *I* can be determined. Similarly, we can also get the value of $E\left[\left(\Delta r(t)\right)^2\right]$ for the CPIC by setting $w_k = 1$ in the MAI estimation stage. Therefore both the APIC and the CPIC receiver have the same BER expression and the only factor that causes their

performance difference is $E\left[(\Delta r(t))^2\right]$. The objective of adopting the adaptive algorithm in the proposed receiver is to reduce the value of $E\left[(\Delta r(t))^2\right]$ in order to improve the performance. The corresponding BER can be found by using Eq. (4.28) and Eq. (4.29), with I_{MAI} replaced by I.

6.4 Numerical Results

In this section, the performance of the MF, the CPIC and the APIC receiver are compared for the asynchronous MC-DS-CDMA system under the fading channel. According to the derivation in the previous section, the BER are calculated, and the plot on BER versus the capacity at an SNR of 20 dB, PG of 32 and $P = M = 2$ is shown in Figure 6.2. These results were obtained based on the assumption of perfect channel estimation and ideal power control is invoked such that each user has equal received power. In the simulations, the step-size and the initial weights for the APIC are set to 0.06 and 1, respectively.

From the figure we can see a good agreement between the theoretical and simulation results. By using the CPIC receiver in the asynchronous MC-DS-CDMA system, the capacity is increased to nearly 4 times as compared to the MF receiver at a BER of 10^{-2}. At the same BER, the APIC receiver is able to accommodate about 10% more users than the CPIC receiver.

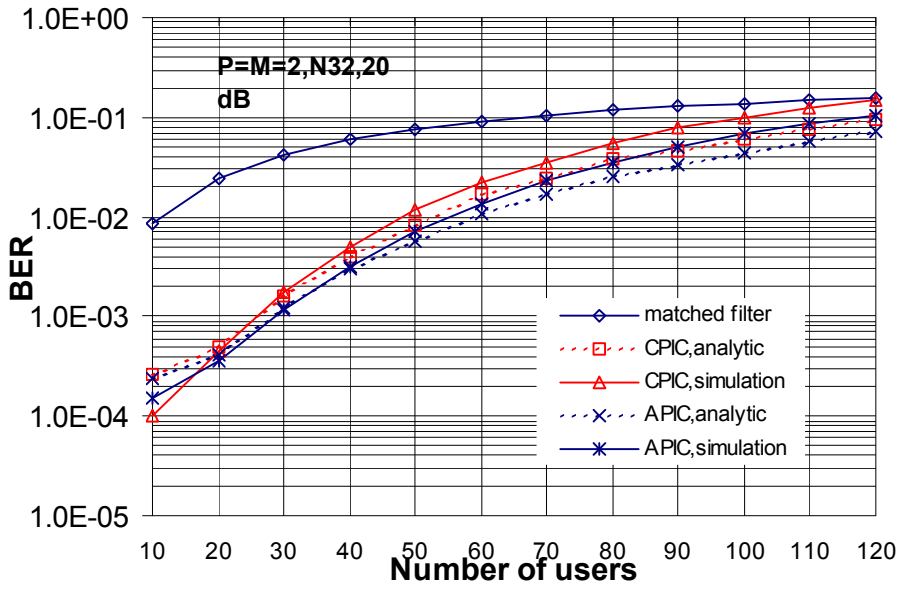

Figure 6. 2 BER performance of various receivers at SNR of 20dB, with P=M=2 and PG =32.

Chapter 7

Conclusions and Directions for Future Research

7.1 Concluding remarks

There is a main theme that has been followed in this thesis.

After taking a historical overview on the development of the wireless communications, the trend of the future mobile communications is obvious: the provision of high data rates through hostile radio communication channels is very essential in order to achieve the goal that anyone can communicate with others from anywhere at any time, and the goal that the worlds of cellular, cordless, low-end wireless LAN, private mobile radio and paging can be unified into one that provides the same type of services everywhere. However, this is difficult to realize since frequency selective fading tends to lead to burst errors in high-speed data transmission.

OFDM is one of the techniques that are robust against frequency selective fading. The combination of OFDM with CDMA amalgamates the advantages of both OFDM and CDMA systems and thus is attractive. Such a system is called multicarrier CDMA. It is believed to be a promising candidate for the 4G mobile communications, which is intended to achieve data rates of up to tens of megabit-per-second, even when used in scenarios such as a vehicle traveling at a speed of up to hundreds of kilometer-per-hour. In this thesis, three types of multicarrier CDMA systems were presented. All these systems are designed to combat multipath selective fading. The parallel

transmission property of these systems is beneficial for increasing the transmitting data rate as well as enlarging the data duration such that the system can be robust against frequency selective fading. System parameters such as the required bandwidth and the subcarrier frequency separation were also compared with each other. Each system has its distinctive features. Whichever system is preferable depends on its individual features. The MC-DS-CDMA system was investigated in this thesis due to its desirable properties such as lesser complexity, the effectiveness for uplink transmission, and the capability for high processing gain which in turn leads to high-quality performance.

Although the MC-DS-CDMA system is stout in combating the multipath selective fading channel, it also inherits the MAI problem from the SC-DS-CDMA systems. Thus, its performance is degraded when the number of users in the system is increased. Surveys on MAI cancellation for SC-DS-CDMA systems were carried out in Chapter 3, which later inspired the receiver design of the MC-DS-CDMA system. Similar to the SC-DS-CDMA system, detectors for MC-DS-CDMA can also be grouped into two basic categories: single-user detectors and multiuser detectors. The matched filter corresponds to the single-user detector. It requires no knowledge beyond the signature waveform and timing of the users it wants to demodulate and treats the interference from other users as additive channel noise. Hence the performance is fairly limited. For the multiuser detector, the receiver has knowledge of the spreading sequence employed by other users and exploits this knowledge for signal detection. The maximum likelihood sequence (MLS) multiuser receiver yields the minimum achievable probability of error, however it is impractical to implement due to its prodigious complexity when the number of users in the system is high. Research focus has been turned to the suboptimal detectors that offer moderate performance with less complexity as compared to the MLS detector. Subtractive interference cancellation

(IC) techniques belong to the suboptimal detection. The basic principle of these schemes is to create estimates at the receiver of the received signals of each individual user in order to subtract out some or all of the interfering signals (MAI) that each user sees. Parallel interference cancellation is one of the most promising multiuser detectors for DS-CDMA systems and such an IC technique with an adaptive MAI estimation stage as well as the diversity combining techniques was proposed for the MC-DS-CDMA system. Simulations as well as the performance analysis of this detection scheme were carried out in this thesis.

The adaptive PIC receiver for the synchronous MC-DS-CDMA system was investigated first. The reason for studying the synchronous case first is based on the simplicity that such an approach can bring about. The exposition and analysis are considerably simplified and the derivation of closed-form expressions becomes easier. Similar trends can usually be found in the analysis of the more complex asynchronous case. Most importantly, synchronous systems are becoming more of practical interest since quasi-synchronous approach has been proposed for satellite and microcell applications. Noting that the MC-DS-CDMA system is originally proposed for a quasi-synchronous channel, it is very appealing to study the synchronous case first. Therefore, great efforts have been poured into the investigation of the synchronous MC-DS-CDMA system in this thesis.

Two methods can be adopted to structure the synchronous APIC receiver, depending on the choice of the reference signal of the adaptive algorithm. One scheme is a subcarrier-based program, which uses the demodulated signal on each subcarrier as the reference and subsequently processes the signals with MRC combining. This structure is adopted in this thesis because it simplifies the structure of the receiver by taking advantage of the synchronization of all users. All users' data arrive at the

receiver without any time offset between each other, thus the signal can be coherently demodulated with only one FFT block. By using the demodulated signal as the reference for the adaptive algorithm, the demand on the subcarriers' reconstruction is avoided. Therefore the cost of building a receiver has significantly been reduced by minimizing the number of IFFT and FFT blocks. The other scheme is to use the composite received signal as the reference of the adaptive algorithm and reconstruct the signals by using K IFFT blocks before the MAI estimation stage. The same number of FFT blocks is needed to re-modulate the signals in the PIC stage. Therefore, this scheme is not so economical although its performance is fairly good.

In the adopted receiver structure, by taking advantage of MRC combining technique before and after the adaptive PIC stage to exploit the frequency diversity provided by the MC-DS-CDMA system, significant performance improvement can be achieved over the matched filter receiver and the conventional PIC receiver. A simple but accurate closed form expression for the bit error rate of this proposed detector was derived. Conditions under which this detector has its best performance were studied thoroughly. Results have shown that the performance can be considerably increased when the appropriate step-size and initial weights are selected. Performance for the multistage detection was also investigated and it was revealed that the advantage of using adaptive PIC beyond the first stage of the multistage interference cancellation structure is only apparent when the level of MAI is high.

Next comes the study for asynchronous detection. The presentation for the asynchronous case has a defferent receiver structures. The reason for a different structure from that of the synchronous case is that the synchronous receiver is a subcarrier-based program, which can use the demodulated signal on each subcarrier as the reference signal for the adaptive algorithm, while in the asynchronous case, such a

scheme becomes impossible due to the time offset between users. The closed form expressions for the performance analysis are also derived and the comparison with the matched filter and the conventional PIC receiver was also presented. Note that in order to simplify the study, conditions such as perfect channel estimation and power control were assumed both in synchronous and asynchronous cases. Further studies may remove these ideal assumptions and thus make the situation more realistic.

7.2 Directions for Future Research

In this thesis, the transmitted chip signals are assumed to be rectangular with unit amplitude. No pulse shaping waveform has been imposed on these signals. The direct effect of this assumption is the overlapping of the frequency spectrum. In some literatures such as [25], [26] and [27], chip wave-shaping filter satisfying the Nyquist criterion is adopted to guarantee the non-overlapping of the DS spectrum. The benefaction of the non-overlapping spectrum is the avoidance of the correlation between subcarriers. However, the frequency spectrum efficiency is also reduced. In this thesis, the correlation between subcarriers has been assumed to be negligible. This is somewhat unrealistic. Although in [27] and some other literatures, it is pointed out that the small correlation coefficients do not result in an obvious worsening of performance, research can still be undertaken to see the effect of the correlation in the proposed schemes.

The channel has been assumed to be frequency non-selective fading on each subcarrier and to fade very slowly. Doppler shift effect does not add too much to the correlation between the subcarriers and neither does it cause severe imperfect channel estimation. This is very important for the proposed schemes since they require perfect channel estimation and the MRC combining is also based on this assumption. It is

possible that the schemes cannot work properly under an imperfect channel estimation condition. It needs more profound investigation in this case to determine how bad this situation would be.

As mentioned previously, there exist two structures of the receiver in the synchronous MC-DS-CDMA system. One is the subcarrier-based program and the other just uses the received signal as the reference signal for the adaptive algorithm. The former scheme was adopted due to its low cost. Our work revealed that the latter scheme shows a fairly better performance over the former one. However, more concrete work needs to be carried out to verify it. It is not difficult to calculate the mean squared error (MSE) of the adaptive PIC receiver for both two structures of the synchronous MC-DS-CDMA system. Hence the performance of the systems may be compared just by using theoretical analysis.

I have always been interested in the *transform domain adaptive algorithm* and had tried to find a way that can take advantage of the FFT block in the MC-DS-CDMA system to improve the performance of the system. This idea comes from the coincidence that the transform domain adaptive algorithm shows a band-partitioning property that is effective in processing correlated input signals [33] and the FFT block in the MC-DS-CDMA system happens to be an orthogonal transform. It is not necessary that the *transform domain adaptive algorithm* is practical for the system. I just bring about the idea that transpired during my research work, hoping that it can give some hints to people who would be interested in this research area.

Appendix A

IFFT Equivalence of Multicarrier Modulation

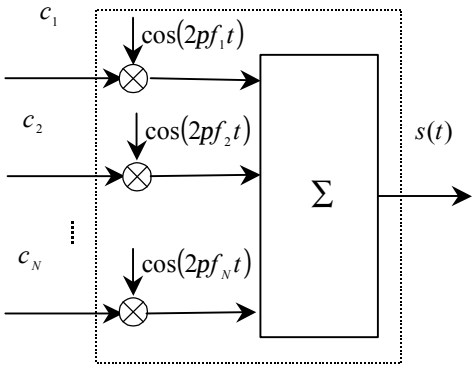

Figure A.1 IFFT equivalence of the multicarrier modulation

Figure A.1 shows an analog multicarrier modulation scheme. The parallel data $\{c_1, c_2 \cdots c_N\}$ are modulated by a set of analog modulators and combined together. This can be implemented by replacing the modulators with an IFFT operation. Denote the frequency separation of successive carriers as Δf, the frequency at each carrier can be expressed as

$$f_n = n \cdot \Delta f, \qquad n = 1, 2, \cdots N \tag{A.1}$$

The composite signal is given by

$$s(t) = \sum_{n=1}^{N} c_n \cos(2\pi f_n t) \tag{A.2}$$

Suppose the symbol duration of c_n is T, and it is sampled with a sampling rate of N

samples per symbol, the *k*th sampling time is given as

$$t_k = \frac{k}{N} T \tag{A.3}$$

The discrete time output signal is given by

$$s(k) \equiv s(t_k) = s(\frac{k}{N} T) = \sum_{n=1}^{N} c_n \cos\left(2pn \frac{k}{N} T\Delta f \right) \tag{A.4}$$

If the frequency separation is $\Delta f = 1/T$, then

$$s(k) = \sum_{n=1}^{N} c_n \cos\left(2pn \frac{k}{N} \right) \tag{A.5}$$

This is the expression of the IFFT operation.

Appendix B

MSE Expression of the MAI Estimation Stage

In this appendix we derive the expression of MSE given by Eq. (4.48). In the MAI estimation stage, the regenerated signals fed into the estimator are given in Eq. (4.14). For the convenience of derivation, we present the equation again in (B1). The *n*th chip corresponding to the *q*th carrier is given by

$$s_q^{(k)}(n) = \sqrt{\frac{P_k}{2M}}\hat{d}_{p,0}^{(k)}c^{(k)}(n)\mathbf{z}_{q,0}^{(k)}, \quad 1 \le m \le M \tag{B.1}$$

and the reference signal is also presented as in Eq. (4.9)

$$r_q(n) = \sum_{k=1}^{K} v_q^{(k)}(n) + h_t(n), \ 0 \le n \le N-1 \tag{B.2}$$

We define the column vector

$$\mathbf{s}(n) = \left[s_q^{(1)}(n) \quad s_q^{(2)}(n) \quad \cdots \quad s_q^{(K)}(n)\right]^T \tag{B.3}$$

where the superscript *T* stands for the transpose.

We also define the $K \times K$ auto-correlation matrix

$$\mathbf{R} = \mathrm{E}\left[\mathbf{s}(n)\mathbf{s}^{\mathrm{T}}(n)\right] \tag{B.4}$$

and the $K \times 1$ cross-correlation vector

$$\mathbf{p} = \mathrm{E}\left[\mathbf{s}(n)r_q^*(n)\right] \tag{B.5}$$

The minimum mean-squared error (MMSE) is given by

$$e_{\min} = E\left[\left|r_q(n)\right|^2\right] - \mathbf{p}^{\mathbf{H}}\mathbf{R}^{-1}\mathbf{p} \tag{B.6}$$

From the assumptions mentioned in chapter 4, we have

$$\mathbf{R} = \begin{bmatrix} \frac{1}{2MN} & 0 & \cdots & 0 \\ 0 & \frac{1}{2MN} & \cdots & 0 \\ \cdots & \cdots & & \cdots \\ 0 & \cdots & & \frac{1}{2MN} \end{bmatrix} = \frac{1}{2MN}\mathbf{I} \tag{B.7}$$

where $\mathbf{I}$ is the unity matrix. The inverse of the matrix $\mathbf{R}$ is given by

$$\mathbf{R}^{-1} = 2MN\,\mathbf{I} \tag{B.8}$$

$$E\left[s_q^{(k)}(n) r_q^*(n)\right] = E\left[\left(\sqrt{\frac{P_k}{2M}}\hat{d}_{p,0}^{(k)} c^{(k)}(n) z_{q,0}^{(k)}\right)\right.$$

$$\left.\cdot\left(\sum_{i=1}^{K}\sqrt{\frac{P_i}{2M}} d_{p,0}^{(i)} c^{(i)}(n)\left[z_{q,0}^{(i)}\right]^* + h_t^*(n)\right)\right] \tag{B.9}$$

From all those assumptions we have made, we can easily have

$$E\left[s_q^{(k)}(n) r_q^*(n)\right] = \frac{1}{2MN} E\left[\left(\hat{d}_{p,0}^{(k)} d_{q,0}^{(k)}\right)\right] \tag{B.10}$$

From Eq. (4.34) and Eq. (4.35),

$$E\left[\hat{d}_{p,0}^{(k)} d_{p,0}^{(k)}\right] = 1 - 2P_{ini}[e] \tag{B.11}$$

Hence,

$$\mathbf{p} = \frac{1 - 2\mathrm{P}_{\mathrm{ini}}[e]}{2MN}\begin{bmatrix}1 & 1 & \cdots & 1\end{bmatrix}^T \tag{B.12}$$

$$E\left[\left|r_q(n)\right|^2\right] = E\left[\left|\sum_{k=1}^{K} v_q^{(k)}(n) + h_t(n)\right|^2\right]$$

$$= \sum_{k=1}^{K} E\left[\left|\sqrt{\frac{P_k}{2MN}} d_{p,0}^{(k)} c^{(k)}(n) z_{q,0}^{(k)}\right|^2\right] + \sigma_h^2$$

$$= \frac{K}{2MN} + \sigma_h^2 \tag{B.13}$$

where $s_h^2 = N_0 / 2$.

From (B.8), (B.12) and (B.13), the expression of the MMSE is given by

$$e_{\min} = \frac{K\left[1-(1-2P_{ini}[e])^2\right]}{2MN} + s_h^2 \tag{B.14}$$

For LMS algorithm [34],

$$MSE = e_{\min} + e_{excess} \tag{B.15}$$

where e_{excess} is the excess MSE and it is proportional to $e_{\min}$. The definition of misadjustment l is the ratio of e_{excess} to $e_{\min}$. With the assumption that the selection of the step-size m makes $l \le 0.1$, we have

$$l = \frac{m\,tr[\mathbf{R}]}{1-m\,tr[\mathbf{R}]} \approx m\,tr[\mathbf{R}] = \frac{mK}{2MN} \tag{B.16}$$

Finally we have the expression of the MSE as

$$\begin{aligned} MSE &= (1+l)e_{\min} \\ &= \left(1+\frac{mK}{2MN}\right)\left\{\frac{K\left[1-(1-2P_{ini}[e])^2\right]}{2MN} + s_h^2\right\} \end{aligned} \tag{B.17}$$

Appendix C

Generation of long sequence codes by IMT2000 Standard

The long scrambling sequences $c_{long,1,n}$ and $c_{long,2,n}$ are constructed from position wise modulo 2 sum of 38400 chip segments of two binary *m*-sequences generated by means of two generator polynomials of degree 25. Let x, and y be the two *m*-sequences respectively. The x sequence is constructed using the primitive (over GF(2)) polynomial $X^{25}+X^{23}+1$. The y sequence is constructed using the polynomial $X^{25}+X^{3}+X^{2}+X+1$. The resulting sequences thus constitute segments of a set of Gold sequences. The sequence $c_{long,2,n}$ is a 16777232 chip shifted version of the sequence $c_{long,1,n}$.

Let $n_{23}\cdots n_0$ be the 24 bit binary representation of the scrambling sequence number n with n_0 being the least significant bit. The x sequence depends on the chosen scrambling sequence number n and is denoted x_n, in the sequel. Furthermore, let $x_n(i)$ and $y(i)$ denote the *i*th symbol of the sequence x_n and y, respectively.

The *m*-sequences x_n and y are constructed as:

Initial conditions:

$$x_n(0)=n_0,\ x_n(1)=n_1,\cdots,\ x_n(22)=n_{22},\ x_n(23)=n_{23,}\ x_n(24)=1. \qquad \text{(C.1)}$$

$$y(0)=y(1)=\cdots y(23)=y(24)=1. \qquad \text{(C.2)}$$

Recursive definition of subsequent symbols:

$$x_n(i+25) = x_n(i+3) + x_n(i) \mod 2,\ i = 0, \cdots, 2^{25} - 27, \tag{C.3}$$

$$y(i+25) = y(i+3) + y(i+2) + y(i+1) + y(i) \mod 2,\ i = 0, \cdots, 2^{25} - 27. \tag{C.4}$$

Define the binary Gold sequence z_n by

$$z_n(i) = x_n(i) + y(i) \mod 2, \quad i = 0, 1, 2, \cdots, 2^{25} - 2. \tag{C.5}$$

The real valued Gold sequence Z_n is defined by

$$Z_n(i) = \begin{cases} +1 & if\ z_n(i) = 0 \\ -1 & if\ z_n(i) = 1 \end{cases} \quad \text{for } i = 0,1,\ldots,2^{25} - 2. \tag{C.6}$$

Now, the real-valued long scrambling sequences $c_{long,1,n}$ and $c_{long,2,n}$ are defined as follows:

$$c_{long,1,n}(i) = z_n(i), \quad i = 0, 1, 2, \cdots, 2^{25} - 2 \tag{C.7}$$

$$c_{long,2,n}(i) = z_n\left((i + 16777232) \bmod \left(2^{25} - 1\right)\right),\ i = 0, 1, 2, \cdots, 2^{25} - 2. \tag{C.8}$$

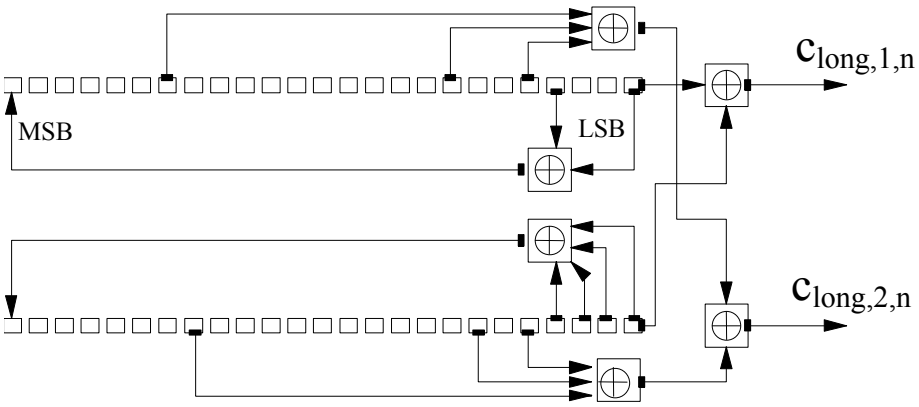

Figure C.1 Configuration of scrambling sequence generator

Appendix D

Jakes Model and its relationship with Rayleigh density formula

In the classical papers by Clarke [39] and Jakes [40], a statistical description of the mobile radio channel is developed. The model treats a scenario where N plane waves are arriving at the receiver from random directions. The different propagation paths cause the waves to have different attenuation and phase shifts. The phases of the waves are uniformly distributed from 0 to $2p$. The amplitudes and phases are assumed to be statistically independent.

As have been pointed out in [40], experiments have shown that the envelope of the mobile radio signal is Rayleigh distributed when measured over distances of a few tens of wavelengths where the mean signal is sensibly constant. This suggests the assumption, reasonable on physical grounds, that at any point the received field is made up of a number of horizontally traveling plane waves with random amplitudes and angles of arrival for different locations. A diagram of this simple model is shown in Figure D.1 with plane waves from stationary scatterers incident on a mobile traveling in the *x*-direction with velocity *v*. The *x*-*y* plane is assumed to be horizontal. The vehicle motion introduces a Doppler shift in every wave:

$$w_n = \frac{2p}{l} v \cos a_n \qquad \text{(D.1)}$$

l being the wavelength of the transmitted carrier frequency.

The expression that represents the field as a superposition of plan waves is given by [40]:

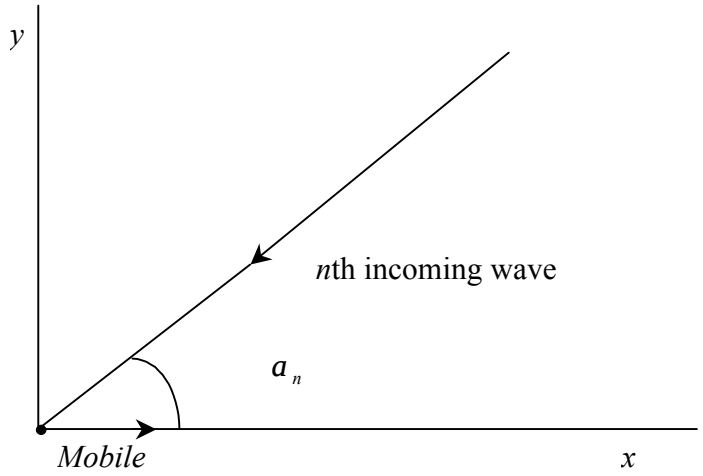

Figure D.1 A typical component wave incident on the mobile receiver.

$$E(t) = \Re\left[T(t)e^{iw_c t}\right], \tag{D.2}$$

where

$$T(t) = E_0 \sum_{n=1}^{N} c_n e^{i(w_m t \cos a_n + j_n)}, \tag{D.3}$$

and

$$c_n^2 = p(a_n)da = \frac{1}{2p}da \ . \tag{D.4}$$

$w_m = \frac{2p}{l}v$ being the maximum Doppler shift and $p(a_n)$ being the pdf of the random variables a_n.

Under the assumption that the arrival angles are uniformly distributed with $da = 2p / N$, the values of c_n^2 and a_n are given by

$$c_n^2 = 1/N, \tag{D.5}$$

$$a_n = \frac{2pn}{N}. \tag{D.6}$$

If N is large enough, the Central Limit Theorem (CLT) can be invoked to conclude that $T(t)$ is approximately a complex Gaussian process, so that $|T|$ is Rayleigh as desired. Research has revealed that the Rayleigh approximation is quite good for $N \geq 6$.

Denoting the envelope as r, i.e., $r = |T|$, the probability density of r is

$$p(r) = \begin{cases} \frac{r}{b} e^{-r^2/2b}, & r \geq 0 \\ 0, & r < 0 \end{cases} \tag{D.7}$$

which is the Rayleigh density function and $b = E_0^2 / 2$ in this formula.

Publication List

[1]. Huahui Wang, Kai Yen, Kay Wee Ang and Yong Huat Chew, "Performance analysis of an adaptive PIC receiver for asynchronous multicarrier DS CDMA system," to *IEEE International Symposium on Personal, Indoor, and Mobile Radio Communications (PIMRC) 2003*, China: Beijing, pp.1835-1839.

[2]. Huahui Wang, Kay Wee Ang, Kai Yen and Yong Huat Chew, "An adaptive PIC receiver with diversity combining for multicarrier DS CDMA system," *IEEE 50th Vehicular Technology Conference (VTC)-Fall 2003*, USA: Orlando, Florida, October 2003.

[3]. Huahui Wang, Kai Yen, Kay Wee Ang and Yong Huat Chew, "Performance Analysis of an Adaptive PIC Receiver with Diversity Combining for Multicarrier DS-CDMA System," to appear in VTC-Spring 2004.

[4]. Huahui Wang, Kai Yen, Kay Wee Ang and Yong Huat Chew, "Adaptive Parallel interference cancellation receiver for synchronous multicarrier DS CDMA system," Submitted to *IEEE Trans. Commun.*.

Bibliography

[1]. T. S. Rappaport, *Wireless communications: Principles and Practice*, Prentice Hall, 1996.

[2]. J. E. Padgett, C. G. Gunther, T. Hattori, "Overview of wireless personal communications," *IEEE Commun. Mag*. pp. 28-41, Jan. 1995.

[3]. J. Uddenfeldt, "Digital cellular – Its roots and its future," *Proc. of IEEE*, Vol. 86, no. 7, Jul 1998.

[4]. X. Gui and T. S. Ng, "Performance of asynchronous orthogonal multicarrier CDMA system frequency selective fading channel," *IEEE Trans. Commun.,* Vol. 47. no.7, pp.1084-1091, Jul. 1999.

[5]. N. Morinaga, M. Nakagawa and R. Kohno, "New concepts and technologies for achieving highly reliable and high-capacity multimedia wireless communications systems," *IEEE Commun. Mag.,* pp.34-40, Jan. 1997

[6]. E. Sourour and M. Nakagawa, "Performance of orthogonal multi-carrier CDMA in a multipath fading channel," *IEEE Trans. Commun.,* Vol. 44. no. 3, pp.356-367, Mar. 1996.

[7]. J. S. Lee and L. E. Miller, *CDMA Systems Engineering Handbook*, Artech House Publishers, 1998.

[8]. S. B. Weinstein and P. M. Ebert, "Data transmission by frequency-division multiplexing using the discrete Fourier transform," *IEEE. Trans. Commun. Technol.*, vol. COM-19, pp. 628-634, Oct. 1971.

[9]. L. J. Cimini Jr., "Analysis and simulation of a digital mobile channel using orthogonal frequency division multiplexing," *IEEE Trans. Commun*. Vol. COM-33, pp. 665-675, July 1985.

[10]. J. A. C. Bingham, "Multicarrier modulation for data transmission: An idea whose time has come," *IEEE Commun. Mag.,* vol. 28, pp. 5-14, May 1990.

[11]. N. Yee, J-P. Linnartz and G. Fettweis, "Multicarrier CDMA in Indoor Wireless Radio Networks," *Proc. of IEEE PIMRC'93*, Yokohama, Japan, pp.109-13, Sept. 1993.

[12]. V. M. DaSilva and E. S. Sousa, " Performance of Orthogonal CDMA Codes for Quasi-Synchronous Communication Systems," *Proc. of IEEE ICUPC'93*, Ottawa, Canada, pp. 995-99, Oct. 1993.

[13]. L. Vandendorpe, "Multitone Direct Sequence CDMA System in an Indoor Wireless Environment," *Proc. of IEEE First Symposium of Communications and Vehicular Technology in the Benelux, Delft, The Netherlands,* pp 4.1.1-4.1.8, Oct. 1993.

[14]. S. Hara and R. Prasad, "Overview of Multicarrier CDMA", *IEEE Commun Mag.*, Vol. 35, pp. 126-133, Dec. 1997.

[15]. J. G. Proakis, *Digital Communications*. New York: McGraw-Hill, 1966.

[16]. A. Due-Hallen, J. Holzman, and Z. Zvonar, "Multiuser detection for CDMA systems," *IEEE Personal Communications*, pp. 46-58, Apr 1995.

[17]. S. Verd?, *Multiuser detection*, New York, NY: Cambridge University Press, 1998.

[18]. S. Moshavi, "Multi-user detection for DS-CDMA communications," *IEEE Commun Mag*., pp124-136, Oct. 1996

[19]. S. Verd?, "Minimum probability of error for asynchronous Gaussian multiple-access channels," *IEEE Trans. Info. Theory*, vol. IT-32, no. 1, pp. 85-96. Jan 1986.

[20]. D. Divsalar, M. K. Simon, and D. Raphaeli, "Improved parallel interference cancellation for CDMA," *IEEE Trans. Commun*. Vol. 46, pp.258-268, Feb, 1998.

[21]. P. Patel and J. Holtzman, "Performance comparison of a DS/CDMA system using a successive interference cancellation (IC) scheme and a parallel IC scheme under fading," *IEEE Proc. ICC'94*, pp.510-514, 1994.

[22]. G. Xue, J. Weng, Tho Le-Ngoc, and S. Tahar, "Multiuser detection techniques: an overview," Dept of ECE, Concordia Univ. Oct. 1998.

[23]. M. Kavehrad and P. J. McLane, "Performance of low complexity channel coding and diversity for spread spectrum in indoor wireless communications," AT&T Tech. J. vol. 64, no.8, pp, 1927-1965, Oct. 1985.

[24]. G. L. Turin, " Introduction to spread-spectrum antimultipath techniques and their application to urban digital radio," *Proc. IEEE,* vol. PROC-68, no. 3, pp. 328-353, Mar. 1980.

[25]. W. Xu and L. B. Milstein, "On the performance of multicarrier RAKE systems", *IEEE Trans. Commun*., vol. 49, pp. 1812-1823, Oct. 2001.

[26]. S. Kondo and L.B. Milstein, "Performance of multicarrier DS CDMA systems," *IEEE Trans. Commun*., vol. 44, pp. 238-246, Feb. 1996.

[27]. F. Lin and L. B. Milstein, "Successive interference cancellation in multicarrier DS/CDMA", *IEEE Trans. Commun*., vol. 48, no. 9, pp. 1530-11540, Sept. 2000.

[28]. M. K. Varanasi and B. Aazhang, "Near-optimum detection in synchronous code-division multiple-access systems," *IEEE Trans. Commun*., vol. 39, pp. 725-736, May. 1991.

[29]. G. Xue, J. Weng, Tho Le-Ngoc, and S. Tahar, "Adaptive multistage parallel interference cancellation for CDMA," *IEEE J. Select. Areas Commun*., vol. 17, No.10, pp. 1815-1827, Oct. 1999.

[30]. W. Xu, L. B. Milstein, "Performance of multicarrier DS CDMA systems in the presence of correlated fading", *in Proc. VTC'97,* vol. 3, pp. 2050-2054, May 1997.

[31]. S. Haykin, *Adaptive Filter Theory*. Prentice Hall, 3rd ed., 1996.

[32]. Y. C. Yoon, R. Kohno and H. Imai, "A spread-spectrum multiple access system with cochannel interference cancellation for multipath fading channels," *IEEE J. Select. Areas Commun.,* vol. 11, pp. 1067-1075, Sept. 1993.

[33]. B.Farhang-Boroujeny, *Adaptive Filters: Theory and Application,* John Wiley & Sons, 1999.

[34]. M. C. Jeruchim, P. Balaban and K. S. Shanmugan, *Simulation of Communication Systems*. New York: Plenum, 1994.

[35]. R. Lupas and S. Verd?, “Near-far resistance of multiuser detectors in asynchronous channel,” *IEEE JSAC*, vol. SAC-10, no.2, pp. 328-343, Feb. 1992.

[36]. A. Kajiwara and M. Nakagawa, “Microcellular CDMA system with a linear multiuser inteference cancellation,” *IEEE JSAC*, vol. 12, no. 4, pp. 605-611, May 1994.

[37]. R. K. Morrow, JR. and J. S. Lehnert, “Bit-to-bit error dependence in slotted DS/SSMA packet systems with random signature sequences,” *IEEE Trans. Commun*., vol. 37, no. 10, pp. 1052-1061, Oct.. 1989.

[38]. D.E. Borth and M.B. Pursely, “Analysis of direct sequence spread spectrum multiple access communication over Rician fading channels,” *IEEE Trans. Commun*., vol. COMM-27, no. 10, pp. 1566-1577, Oct. 1979.

[39]. R. H. Clarke, “A statistical theory of mobile-radio-reception,” *The Bell System Technical Journal*, 47(6): 57-1000, July-August 1968.

[40]. Jr W.C.Jakes, Multipath interference, in Jr W. C. Jakes, editor, *Microwave Mobile Communications*, IEEE Piscataway, NY 1974.

[41]. S. Stein, “Linear diversity combining techniques,” in *Communication Systems and Techniques*. New York: McGraw-Hill, 1966, ch. 10.

[42]. J. N. Pierce and S. Stein, “Multiple diversity with nonindependent fading,” *Proc. IRE*, vol. 48, pp. 89-104, Jan. 1960.

[43]. M. Pursley, “Performance evaluation for phase-coded spread-spectrum multiple access communications -- Part I: System analysis,” *IEEE Trans. Commun.,* vol. COMM-25, no. 8, pp. 795-799, Aug. 1977.